NPL REPORT IR 40

A PRACTICAL APPROACH TO REPORT OUTPUT FACTORS FOR THE NPL BEAM DATA ACQUISITION SERVICE. EMPHASIS IN SMALL FIELDS

NAME OPF AUTHOR(S): I SILVESTRE, A SUBIEL, A DIMITRIADIS, S DUANE, J SNAITH, M HOMER

DECEMBER 2016

A practical approach to report output factors for the NPL Beam Data Acquisition Service. Emphasis in Small Fields

I Silvestre, A Subiel, A Dimitriadis, S Duane, J Snaith, M Homer,
Acoustic and Ionizing Radiation Division

ABSTRACT

As part of Pinnacle treatment planning commissioning, a practical approach to report output factors for small fields (0.5 x 0.5 up to 3 x 3 cm^2) using the Daisy-chain was investigated. Experimental field size and detector specific factors were also determined. Comparison between the two methods was reported. Output factors for all the relevant field sizes (ranging from 0.5 x 0.5 up to 40 x 40 cm^2) were determined for the NPL Linac with the Agility head. The results allow for a set of reference data that are useful for comparison with measurements performed during the NPL beam data acquisition service RD18, for similar linacs and conditions as the ones reported here.

ISSN 1754-2952

National Physical Laboratory
Hampton Road, Teddington, Middlesex, TW11 0LW

Approved on behalf of NPLML by
Giuseppe Schettino, KL AIR.

CONTENTS

1 INTRODUCTION

Small field dosimetry is still an area of research, where the medical physics community is looking for a consensus. Between 2013 and 2016, medical physics related journals published approximately 50 papers considering different aspects of small field dosimetry for high energy photon beams[1]. Some of these studies reflect the fact that is possible to determine corrections to detector readings that are specific to the combination of field size, detector, linac type and measurement conditions. Several groups worldwide are presently working on the development of comprehensive dosimetric protocols for dose measurements in small fields [1] [2]. Therefore, it is still possible for individual institutions to establish their own procedures based on their experience and the equipment available.

The purpose of this work was to establish a workflow that, from a practical point of view, would comply with small field dosimetry theory, and would offer confidence in the measurement of small field output factors (down to a nominal 0.5 x 0.5 cm^2) with the detectors available at NPL. Additionally, the objective of this work was to characterize output factors (OPF) of the NPL's linac B in the range of field sizes required by Pinnacle treatment planning system (TPS).

Small field dosimetry has been associated with several patient dose delivery errors [3]. Any efforts to generate local practical approaches for small field measurements are of great value. It will increase the confidence in the results as well as the consistency in the characterization of beam parameters of relevance for TPS commissioning and linac QA in the range of small fields.

2 METHODS AND MATERIALS

2.1 NPL-ELEKTA LINAC.

NPL-Elekta linac B is a Versa HD model with an Agility MLC enabling flattened (FF) and unflattened (FFF) beams. The linac has the capability to provide a full set of X-ray energies. However, for the purpose of this work only 6 MV, 10 MV, 6 MV FFF and 10 MV FFF beams have been used.

Field sizes ranging from 0.5 x 0.5 cm^2 to 40 x 40 cm^2 cm were organized in a Stored Beam Sequence (a feature available at the linac console) to make the measurements more efficient.

2.2 DETECTORS

A total of 7 detectors were used to carry out the measurements.

Table 1 provides the characteristics of the diodes and other solid state detectors used in this work.

The properties of the ionization chambers (IC) that are relevant to output factor determination are given in **Note 1** *Dimensions relevant to sensitive volume. Volume in mm3*
Note 2 *As stated in the manufacturer's certificate*
Note 3 *For this work, the mark on the cap provided by the manufacturer was used to position the detector vertically*
Table 2**.** The table includes chambers that are unsuitable for small field measurements. Those detectors were employed to determine OPF for a set of field sizes ranging from 4 x 4 cm^2 to 40 x 40 cm^2. More than one detector was used in that range in order to establish the repeatability of the measurements in relation to the positioning setup and also to demonstrate the consistency of the OPF values for larger field sizes independently of the detector sensitive volume.

1 Web of science review for PUBLICATION NAME: (medical physics, physics in medicine and biology and journal of applied clinical medical physics); TOPIC: (small field dosimetry) and YEARS: 2013, 2014, 2015, 2016.

Table 1. Diode and solid state detectors description.

Detector	Dimensions [mm][1]	Sensitive Material	Effective measurement point [mm]	Wall material	Material density [g/cm^3]	Electron density [e$^-$/g] relative to water
IBA SFD diode	Thickness 0.06, ∅ 0.6 (0.017mm^3)	Silicone	0.66[2]	ABS + epoxy resin	2.33	0.901
PTW E diode 60012	Thickness 0.025, ∅ 1.13 (0.025 mm^3)	Silicone	0.6	RW3 + epoxy resin	2.33	0.901
Exradin W1 scintillator	Thickness 3, ∅ 1.0 (2.3mm^3)	Polystyrene	~3.5[3]	ABS plastic enclosure	1.05	0.975

Note 1 *Dimensions relevant to sensitive volume. Volume in mm^3*
Note 2 *As stated in the manufacturer's certificate*
Note 3 *For this work, the mark on the cap provided by the manufacturer was used to position the detector vertically*

Table 2. Ionization chambers description.

Detector	Dimensions [mm][1]	Wall	Central electrode	Wall thickness [g/cm^2]
PTW 30013 Farmer	Cavity length 23.0, ∅ 6.1 (0.6cm^3)	Graphite + PMMA	Aluminium	0.056
PTW 31010 Semiflex	Cavity length 6.5, ∅ 5.5 (0.125cm^3)	Graphite + PMMA	Aluminium	0.078
IBA CC13	Cavity length 5.8, ∅ 6.0 (0.13cm^3)	C-552	C-552	0.070
Exradin A26 micro chamber	Cavity length 3.3, ∅ 3.3 (0.015cm^3)	C-552	C-552	0.070

Note 2 *Dimensions relevant to sensitive volume. Volume in cm^3*

2.3 MEASUREMENT SET UP

For each energy, TPR (beam index quality) and output in reference conditions, i.e. for 10 x 10 cm^2 field, Source Surface Distance (SSD) of 95 cm and depth of 5 cm were measured using a PTW 30013 Farmer chamber (S/N 03981). Measurements were performed in a water phantom with the beam at 0^o gantry angle, chamber axis perpendicular to the beam axis and its geometrical centre at the depth of interest. To provide reassurance that the size of the detector does not greatly affect the value of the TPR10, which is the reference dose for Pinnacle in our conditions, the values of dose for 95cm SSD, 5cm depth and for 90cm SSD and 10cm depth were also measured with different ionization chambers with various dimensions of sensitive volume.

All the OPF measurements were performed in water at 90 cm SSD and 10 cm depth.

Prior to the measurements, each detector was aligned to the linac crosshairs (using alignment caps or detector marks). To determine the OPF and for each energy and every detector, inline and crossline profiles were acquired. IBA Blue phantom and OmniPro Accept v7.4 were used to determine the central axis position based on the central axis correction (CAX) and the radiation field sizes. For field sizes ranging from 4 x 4 cm^2 to 40 x 40 cm^2, the detectors were centred using the 10 x 10 cm^2 field.

For small field sizes (from 0.5 x 0.5 cm^2 to 3 x 3 cm^2), inline and crossline scans were measured for each of the nominal fields. The signal from the linac monitor ionization chamber connected to the IBA Blue phantom was used as the reference detector. This setup avoided interference from any other detector in the small field. Each detector was positioned accordingly to its specific CAX.

With all the detectors except for the Exradin W1 (it uses a two channel electrometer SuperMax), the dose measurements were acquired with a Scanditronix Welhofer Dose 1 electrometer (S/N 05-9626).

In the specific case of the W1 detector, it is not possible to measure scans of relative dose. The dual channel measurements are not fully integrated into any of the 3D scanners solutions. We used the precision positioning system from the IBA system (0.1 mm positioning error) to move the detector inline and crossline to determine the position of the radiation field centre. Due to insufficient time to perform measurements, for all field sizes, only the smallest and most critical field, i.e.: 0.5 x 0.5 cm^2, was manually scanned (inline and crossline) for all the energies. The profiles were measured between ± 10 mm with 1 mm resolution in the tails and 0.1 mm in the rest of the regions of the field. Values for channel 1 signal (SC1) from the SuperMax electrometer (acquired in continuous mode for 5 seconds) were plotted.

CAX shifts were individually applied for each beam. In order to save time and to avoid confusion; the IBA Blue phantom (0,0) position as per the initial alignment (with cap/detector mark), was kept the same. The detectors were moved one at a time to the measured radiation centre for each beam energy.

2.3.1 Exradin W1 scintillator detector, CLR determination.

A special setup was used to measure Cerenkov Light Ratio (CLR) and output factors with the Exradin W1 scintillator detector. The recommendations from Underwood *et al.* [4] were followed.

The detector was positioned with the longitudinal axis parallel to the beam and the effective point of measurement aligned against the mark on the positioning cap provided by Standard Imaging (x, y and z = 0). The fibre optic cable was guided and fixed towards one of the bottom corners of the tank following one of the diagonals of the field. Inline and crossline profiles for 0.5 x 0.5 cm^2 field were measured in order to align the scintillator.

For relatively large fields, it can be assumed that:

$$\frac{(Scintillator\ Measurement)_{test}}{(Scintillator\ Measurement)_{ref}} = \frac{(Ion\ Chamber\ Measurement)_{test}}{(Ion\ Chamber\ Measurement)_{ref}} \quad (1)$$

The general formula for acquiring measurements with the W1, the SuperMax electrometer and the dual channel procedure is given by:

$$Scintilator\ Measurement\ (Dose) = Gain \times (SC1 - SC2 \times CLR) \quad (2)$$

From equations (1) and (2) one can derive the CLR value, which can be expressed as:

$$CLR = \frac{(Ion\ Chamber)_{test}\ \times SC1_{ref} - (Ion\ Chamber)_{ref}\ \times SC1_{test}}{(Ion\ Chamber)_{test}\ \times SC2_{ref} - (Ion\ Chamber)_{ref}\ \times SC2_{test}} \quad (3)$$

The ionization chamber used for these measurements was the PTW 31010 semiflex (S/N 4042). The reference and "test" fields were 10 x 10 cm^2 and 4 x 4 cm^2, respectively. To investigate the robustness of the approach, the 5 x 5 cm^2 field was also used as a "test" field.

2.4 OUTPUT FACTOR CALCULATION

2.4.1 Field sizes from 4 x 4 cm^2 to 40 x 40 cm^2

The Output factors for this group of fields were measured with the ionization chambers: PTW Farmer type 30013 (S/N 03981), PTW semiflex 31010 (S/N 4042) and the IBA CC13 (S/N 93900).

By definition, and when measuring with an ionization chamber, output factors are defined as the ratio of dose for a given field size (test) and the reference field, in this case the 10 x 10 cm^2 field.

$$OPF_{test} = \frac{M_{test} \times k_{TPtest} \times N_{Dw} \times f_{elec} \times f_{ion}}{M_{10x10} \times k_{TP10x10} \times N_{Dw} \times f_{elec} \times f_{ion}} \tag{4}$$

where:
$M_{test} = \ charge\ readings\ in\ the\ test\ field\ [nC]$
$k_{TPtest} = correction\ for\ pressure\ and\ temperature\ variation\ from\ standard\ conditions$
$M_{10x10} = \ charge\ readings\ in\ the\ test\ field\ [nC]$
$k_{TP10x10} = correction\ for\ pressure\ and\ temperature\ variation\ from\ standard\ conditions$
$N_{Dw} = ionization\ chamber\ calibration\ factor$
$f_{elec} = electrometer\ correction\ factor$
$f_{ion} = correction\ for\ ion\ recombination$

For beams, field sizes and detectors, where the readings of charge are not affected by volume averaging effects, or density of the sensitive volume related variations of the detector's response, the OPF can be determined using the ratio of the detector readings corrected for the ambient conditions.

$$OPF_{test} = \frac{M_{test} \times k_{TPtest}}{M_{10x10} \times k_{TP10x10}} \tag{5}$$

2.4.2 Field size definition for small fields: nominal vs. Effective Field Size (EFS).

According to Charles *et al.* [5], for field sizes larger than 4 x 4 cm^2, an error of 1 mm in the definition of the field size will not have an important effect on the OPF value. Two major components affecting the field size definition for small fields are collimator and detector position errors. Charles *et al.* [5] have demonstrated that collimator positioning errors have a major impact on the OPF value and showed that for fields smaller than 1.5 x 1.5 cm^2, a change in 1 mm on the total field size leads to a variation of 1% in the output factor. These results vary with size of the detector and the energy of the beam.

In our work, in order to account for the effect of the collimator position, we acquired inline and crossline profiles for fields ranging from 0.5 x 0.5 cm^2 to 3.0 x 3.0 cm^2 with four different detectors: Exradin A26 micro IC, IBA SFD diode, PTW E diode 60012 and EBT XD films. The effect of the detector sensitive volume on the results was analysed. We used the field size definition given by Crammer-Sargison *et al.* [6]:

$$FS_{eff} = \sqrt{A \times B} \tag{6}$$

where:
A and B correspond to the inplane and crossplane dosimetric field size (defined as the FWHM at 50% of the isodose level or at the position of the maximum slope for FFF beams).

2.4.3 Daisy chain

The sizes of small field we considered in this work ranged between 0.5 x 0.5 cm^2 and 3 x 3 cm^2. In the particular case of silicon detectors it is necessary to compensate for their over-response to field-size dependent changes in the low-energy component of the photon spectrum due to secondary scatter [7]. In order to minimise energy and field size dependence in the response of the silicon diodes used in our work, the field of 4 x 4 cm^2 was considered as the intermediate field in which the silicon diode would be cross-calibrated against a small or medium size ionization chamber. This procedure enables us to account for the influence of spectral changes between the 10 × 10 cm^2 and the smaller fields. This strategy (by means of which one transfers the normalization of the small field factors from the reference field size through an intermediate field size) is known as "daisy chaining".

Correction factors would be a function of the spectral changes and the detector characteristics for a given measurement configuration (i.e. for a given SSD and depth). Although the Daisy chain is not considered exactly as a correction, from a practical point of view, is expected to provide a general factor to be applied to the measurements with the small silicon diodes. That will allow for the systematic effect related to spectrum variation between a 10 x 10 cm^2 field and a 4 x 4 cm^2 field to be eliminated or diminished.

We determined the ratio of the readings at the reference field size (10 x 10 cm^2) and at an intermediate-sized field (4 x 4 cm^2) using the Exradin A26 micro chamber. Subsequently, we measured factors with two unshielded diodes, IBA SFD diode and PTW E diode 60012, for the 4 x 4 cm^2 field size and the rest of the small fields (0.5 x 0.5, 1 x 1, 2 x 2 and 3 x 3 cm^2). Diode measurements were renormalized to the ion chamber measurements in the reference field, by applying the ratio of the two detector readings at the intermediate field (4 x 4 cm^2). **Equation 7** reflects the measurements involved.

$$OPF(FS_{eff}) \cong \frac{M_{diode}(FS_{eff})}{M_{diode}(4x4cm^2)} \times \frac{M_{IC\ A26}(4x4cm^2)}{M_{IC\ A26}(10x10cm^2)} \tag{7}$$

$$CF = \frac{M_{diode}(10x10cm^2)}{M_{diode}(4x4cm^2)} \times \frac{M_{IC\ A26}(4x4cm^2)}{M_{IC\ A26}(10x10cm^2)} \tag{8}$$

where:
$M_{diode}(FS_{eff})$, $M_{diode}(4x4cm^2)$ and $M_{diode}(10x10cm^2)$ are readings for the small fields, the intermediate field and the reference field with the diode.
$M_{IC\ A26}(4x4cm^2)$, $M_{IC\ A26}(10x10cm^2)$ are readings for the intermediate field and the reference field with the Exradin A26 ionization chamber.

2.4.4 Measurements with Gafchromic EBT-XD films

GAFCHROMIC™ EBT-XD films are designed to determine relative and absolute values of dose. They are particularly suited for measurements in high-energy photons. The optimum dose range for this film type is from 0.4 to 40 Gy. GAFCHROMIC™ EBT-XD film structure is shown in the Figure 1.

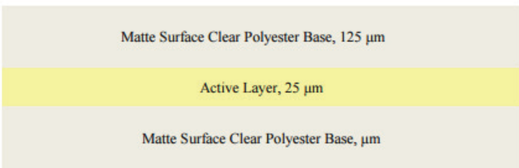

Figure 1. Gafchromic EBT-XD film structure.

According to the manufacturer [8], the film is energy independent with a minimal response difference from 100 keV to the MV range and its composition makes it nearly tissue equivalent. These two main characteristics allows for the film to be considered as an ideal detector to experimentally determine correction factors for other less water equivalent solid state detectors, such as IBA SFD and PTW E 60012 diodes.

Films from the same batch (lot # 5342), were cut into 5 x 5 cm^2 squares. Following manufacturer recommendations, all of the films were scanned in the same (portrait) orientation (long dimension of the film sheet perpendicular to the direction of the scanning). In order to avoid any mistakes in positioning, each piece of film was appropriately marked. The films were digitized with Epson Expression 10000XL scanner (employing Epson Scan ver. 3.49E application) in transmission mode. No colour or sharpness corrections were applied. Films were consistently orientated and positioned in the central part of the scanner's bed. To avoid light dispersion, a black sheet covered all of the unused area of the scanner (see **Figure 2**) and a 4 mm clear glass sheet was used on top of the films to compensate for the gap between the scanner's bed and glass window. A resolution of 150 dpi was selected as it provided an appropriate relation of signal to noise ratio and also manageable file sizes. Films were saved as TIF red-green-blue (RGB) images with 48 bit (16 bit per channel) format.

All films were irradiated at the isocentre in a slab phantom of virtual water WT1, with sufficient backscatter.

For each beam energy (6 MV, 10 MV, 6 MV FFF and 10 MV FFF), films were calibrated with a set of 10 doses ranging from 0 to 4000 cGy delivered with a 10 x 10 cm^2 field. The linac output was measured and MUs necessary to deliver: 50, 100, 200, 450, 750, 1250, 2000, 3000 and 4000 cGy at 95 cm SSD and 5 cm depth were calculated. A piece of an unirradiated film was also included in the calibration curve as a measure of the 0 dose value.

For each energy and for the following field sizes of interest: 0.5 x 0.5, 1 x 1, 2 x 2, 3 x 3, 4 x 4 and 10 x 10 cm^2, the application films were also irradiated in the slab phantom. The conditions for this irradiation were set to SSD 90 cm and 10 cm depth. Linac crosshairs were used to determine the centre of the field for each delivered beam. All application films were irradiated with 1250 cGy.

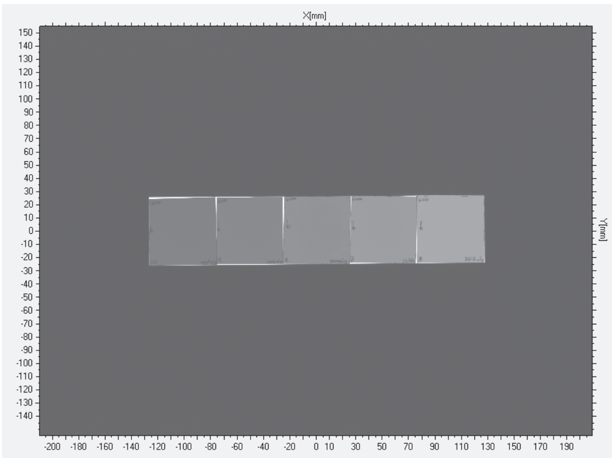

Figure 2 Scanning setup.

Films were analysed with two different commercial softwares: OmniPro IMRT v 1.7 and Verisoft v 5.1.

OmniPro IMRT and Verisoft only use the red channel for the analysis of the RBG scanned films. There was no correction applied for neither the non-uniform response of the scanner nor for lateral response artefacts [9].

After applying the corresponding calibration curve to each of the application films (following the same principles in this study as when measuring with diodes and IC), the radiological centre (RC) of the beam was found by analysing inline and crossline profiles. The ratio of the values of dose in a of 2 x 2 mm^2 ROI, centred at the RC for each small fields and the 10 x 10 cm^2 field size, allowed to calculate the OPFs for the small fields (Equation 9).

$$OPF_{sf\ films} = \frac{Dose_{sf}}{Dose_{10x10}} \quad (9)$$

where:
$Dose_{sf}$ is the value of dose for the ROI in the small field application film
$Dose_{10x10}$ is the value of dose for the ROI in the application film corresponding to the reference 10 x 10 cm^2 field

3 RESULTS

3.1 TPR MEASUREMENTS.

Using the set up explained in section 2.3, a set of base line TPR values were measured for all the beam qualities of interest. Temperature and pressure corrected readings in conditions relevant to TPR calculation are reported. **Table 3** summarises the results obtained.

Table 3 TPR values.

	6MV FF	6MV FFF	10MV FF	10MV FFF
M_{TP} [nC] SSD=90, d=10cm	15.77	15.61	16.60	15.65
M_{TP} [nC] SSD=80, d=20cm	10.77	10.57	12.20	11.32
TPR	0.683	0.677	0.735	0.723

3.1.1 Beam quality index. Detector size influence of FFF beam index quality measurements.

For FFF beams and in the reference 10 x 10 cm^2 field, there is no longer a flat homogeneous region alongside the central axis. The influence of the detector size and its volume effect in the beam index quality determination was therefore assessed.

Measurements with all ionization chambers have been acquired in two conditions: (1) at SSD of 95 cm, and 5 cm depth and (2) at 90 cm SSD and 10 cm depth. At NPL, the first: (1) is the reference condition for beam output calibration for the beams of interest. The second: (2) is the reference condition for Pinnacle TPS. Consequently, in order to try to understand the influence of the detector dimensions on beam quality index determination, those measurements conditions were a good starting point for the analysis.

Table 4 TPR10 values for different sized ionization chambers.

	6 MV	6MV FFF	10 MV	10MV FFF
PTW Farmer	0.852	0.843	0.879	0.866
CC13	0.850	0.846	0.878	0.865
PTW semiflex	0.854	0.843	0.880	0.866
Exradin A26	0.852	0.840	0.876	0.862
Average TPR10	0.852	0.843	0.878	0.865
SDOM	0.0007	0.0011	0.0007	0.0008

The results from **Table 4** show that for FFF beams, there is no a significant difference in the TPR10 value for a given quality measured with ionization chambers with different sensitive volumes. Similar conclusion can be made for non FFF beams. These results are in line with previous work presented by Duane [10]. In the referenced work it was stated that variations in the beam quality index determination for FFF beams, due to variations in chamber response, are unlikely to exceed the accuracy of absolute dose determination in more than 0.5%.

3.2 DETECTOR ALIGNMENT AND EFFECTIVE FIELD SIZE

Placing the detector in the radiation centre of the beam is fundamental for output factor measurements and is even more critical for small fields. As explained in section 2.3, for the set of fields larger than 4 x 4 cm^2, the alignment was performed for each energy and detector (except for the W1), using the 10 x 10 cm^2 field size.

Centring the detector according to positioning caps or detectors' marks, allowed for CAX values smaller than |0.4|mm. This statement does not apply to 6 MV FFF beam, which analysis will be described in more detail further on. The IBA Blue phantom detector positioning accuracy is 0.1mm. Therefore, before switching to the Scanditronix Welhofer Dose 1 electrometer to perform the actual dose measurements, the appropriate CAX was defined and central axis correction was applied. For W1 detector, the alignment was performed just once, using the CAX determined for the 0.5 x 0.5 cm^2 field size.

Figure 3 shows a summary of the alignment scans for the W1 detector. **Table 5** summarises the average CAX found with IBA Omnipro Accept for 3 different field sizes and detectors.

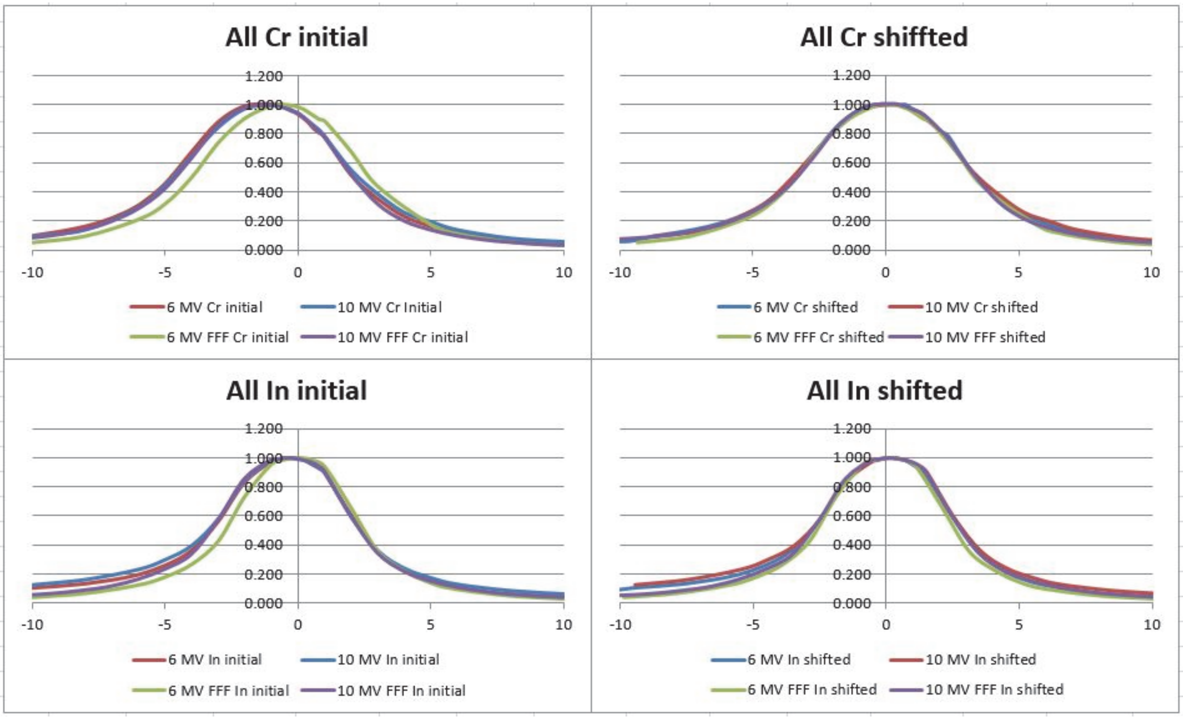

Figure 3 Exradin W1 detector alignment for small field's output factors determination. (inline: In, crossline: Cr)

Table 5 Average CAX for small field alignment with 3 different detectors (Exradin A26, IBA SFD and PTW 60012 unshielded diode), (inline: In, crossline: Cr)

	Average CAX	
	5x5 mm^2	
	Cr	In
6	-0.167	-0.133
10	-0.167	-0.167
6FFF	1.033	0.100
10FFF	-0.233	-0.267
	10x10 mm^2	
6	-0.100	-0.233
10	-0.100	-0.200
6FFF	1.233	0.000
10FFF	-0.167	-0.267
	20x20 mm^2	
6	0.100	-0.067
10	0.000	0.000
6FFF	1.133	0.200
10FFF	-0.300	-0.167

Both results show a feature that had been previously observed in linac B presenting that for the 6 MV FFF beam, more than 1 mm misalignment between the radiation field and the linac crosshairs in the crossline direction is observed. This observation is not relevant to the outcomes described in this report but this finding could lead to future investigations. Particularly for the validation of the MC simulations for FFF and small fields thorough comparison with measurements. If further beam tuning is not performed, one has to be very careful when processing the raw measured scans and especially for 6 MV FFF scans.

The cause for the relatively larger CAX in crossline for 6 MV FFF (in comparison with the rest of the energies) could be due to 1R (primary steering) offset value. Individual beam alignment is crucial to ensure minimal values of CAX.

In relation to the volume average effect, the two diodes and the scintillator used in this study follow Čáp recommendations [11] as to be considered appropriated to measure the smallest nominal field size (in our case 0.5 x 0.5 cm^2). Their diameters in the direction of the scanning are smaller than quarter of the field diameter [12].

It was of interest for this report to investigate the influence of the analysis protocol selected in OmniPro Accept with respect to the findings of the radiological field size.

It is known that high energy photon beams have radial intensity distribution with high intensity in the centre that progressively falls off towards the edge of the field. This is due to its forward distribution nature. For flattened beams this is compensated with the presence of the flattening filters. Field size for FF photon beams are defined at 50% of the FWHM along the central axis. For FFF beams (in the absence of flattening filters) the 50% intensity level occurs at a higher gradient region (sharply descending part) of the beam profile. Therefore, there is a consensus that field sizes for FFF beams does not follow the standard definition.

OmniPro Accept allows the field width to be calculated using a curve width at a user defined percentage value of the central axis dose. By default, the width is defined as the separation between the 50% dose level points. In addition, there is an option to use the maximum slope of left and right sides of the profile for field width calculation (max slope option, Figure 4). According to OmniPro Accept help, the maximum slope option delivers better results for FFF field analysis.

Figure 4 Omnipro Accept different options for field size analysis.

The following tables and figures illustrate the differences between the two approaches. To obtain the Effective Field Size (FS_{eff}), **Equation 6** defined in section 2.4.2 was used. **Table 6a** shows the values of CAX and the observed detail of the misalignment of the radiation centre with the mechanical isocentre (defined by the crosshairs) in the crossline direction for 6 MV FFF. It also shows the calculated values of radiological field sizes using the field definition at 50% of dose level points. Table 6b presents the calculated values of FSeff with all the detectors considered in this part of the experiment. NFS stands for Nominal Field Size.

Table 6a crossline (Cr) and inline (In) radiological Field Size (field width 50%) and CAX

	Exradin A26 [mm] Cr	Exradin A26 [mm] In	Exradin A26 CAX Cr	Exradin A26 CAX In	IBA SFD [mm] Cr	IBA SFD [mm] In	IBA SFD CAX Cr	IBA SFD CAX In	PTW 60012 [mm] Cr	PTW 60012 [mm] In	PTW 60012 CAX Cr	PTW 60012 CAX In
	NFS=5x5 mm^2											
6	7.0	6.9	-0.3	-0.3	6.2	5.3	-0.4	-0.4	6.0	5	0.2	0.1
10	7.2	6.3	-0.3	-0.3	6.3	5.2	-0.2	-0.3	6.1	5.2	0.1	0.1
6 FFF	7.3	6.1	1.0	0	6.5	4.9	0.8	-0.3	6.8	5.1	1.5	0.4
10 FFF	6.9	6.4	-0.6	-0.4	6.1	4.7	-0.3	-0.4	5.8	5.0	0.2	0.0
	NFS=10x10 mm^2											
6	10.9	10.5	-0.3	-0.2	10.5	9.9	-0.3	-0.4	10.4	9.9	0.3	0.0
10	11.2	10.8	-0.2	-0.2	10.8	10.0	-0.2	-0.4	10.6	10.0	0.2	0.0
6 FFF	10.9	10.5	1.1	0.0	10.6	9.4	1.1	-0.2	10.5	9.8	1.6	0.2
10 FFF	11.0	10.7	-0.4	-0.2	10.7	9.7	-0.3	-0.5	10.4	9.9	0.3	-0.1
	NFS=20x20 mm^2											
6	20.6	20.1	-0.1	0.0	20.8	19.8	-0.2	-0.3	20.3	19.5	0.4	0.2
10	20.9	20.1	-0.2	0.1	21.0	19.9	-0.2	-0.3	20.5	19.7	0.3	0.2
6 FFF	20.6	19.9	0.8	0.2	20.9	19.7	1.0	-0.1	20.1	19.5	1.5	0.5
10 FFF	20.7	20.0	-0.4	-0.1	20.9	19.8	-0.5	-0.4	20.4	19.5	0.1	0.1

Table 6b Effective Field Size (field width: 50%) (including EBT-XD Films)

	FS_{eff} [mm]							
	Exradin A26	IBA SFD	PTW 60012	Films	Average/4[(1)]	SD[(3)]	Average/3[(2)]	SD
	NFS=5x5 mm^2							
6 MV	6.95	5.73	5.48	5.80	5.99	0.79	5.67	0.18
10 MV	6.73	5.72	5.63	5.74	5.96	0.61	5.70	0.06
6 MV FFF	6.67	5.64	5.89	5.67	5.97	0.54	5.73	0.17
10 MV FFF	6.65	5.35	5.39	5.67	5.76	0.74	5.47	0.02
	NFS=10x10 mm^2							
6 MV	10.70	10.20	10.15	10.09	10.28	0.31	10.14	0.03
10 MV	11.00	10.39	10.30	10.38	10.52	0.38	10.36	0.07
6 MV FFF	10.70	9.98	10.14	10.18	10.25	0.38	10.10	0.11
10 MV FFF	10.85	10.19	10.15	10.03	10.30	0.39	10.12	0.03
	NFS=20x20 mm^2							
6 MV	20.35	20.29	19.90	19.94	20.12	0.25	20.04	0.28
10 MV	20.50	20.44	20.10	20.14	20.29	0.22	20.23	0.25
6 MV FFF	20.25	20.29	19.80	19.89	20.06	0.27	19.99	0.35
10 MV FFF	20.35	20.34	19.94	19.94	20.14	0.23	20.08	0.28

(1) Average of FS_{eff} determined by the four detectors, (2) Average FS_{eff} with the two diodes and the film,
(3) SD: Standard Deviation

Figure 5 summarises the differences in the FS_{eff} determined with the Exradin A26 IC, the IBA SFD and the PTW 60012 diodes against the "true field size" as determined by the high spatial resolution detector: the EBT film.

Tables 7a and b summarize the calculated values of radiological field sizes for FFF beams using the field definition at the point of maximum slope as well as the calculated values of FS_{eff} with all the detectors considered in this part of the experiment.

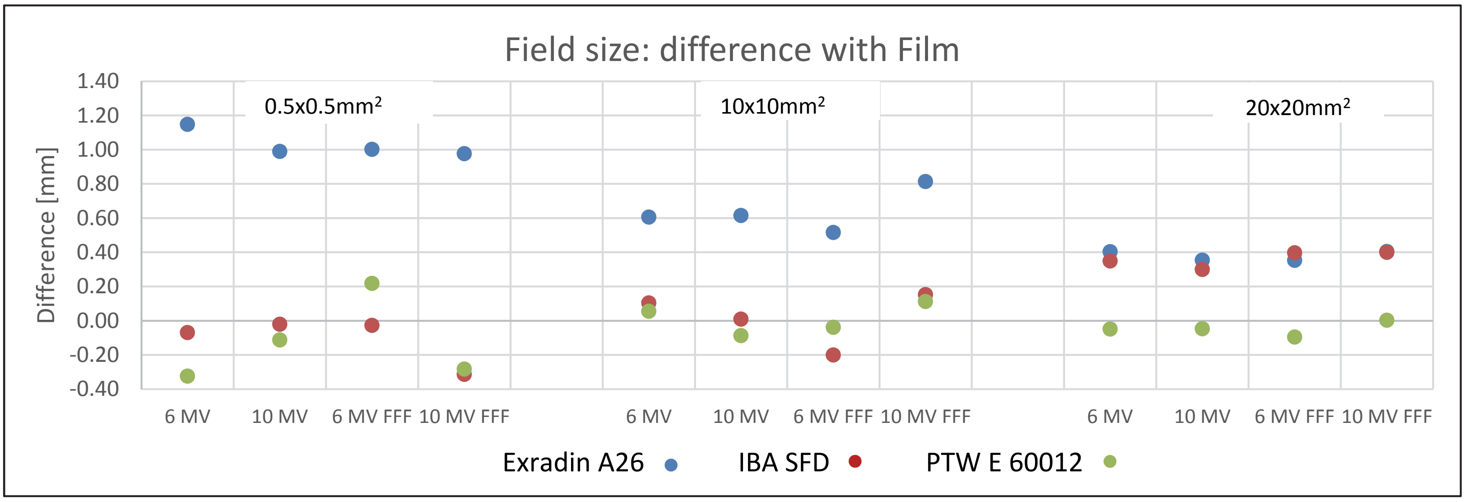

Figure 5. Effective Field Size: Comparison between different detectors.

Table 7a Cr and In radiological Field Size (field width: max. slope).

	Exradin A26 [mm]		IBA SFD [mm]		PTW 60012 [mm]	
	NFS=5x5 mm^2					
	Cr	In	Cr	In	Cr	In
6 MV FFF	4.5	6.0	5.1	3.9	4.9	3.6
10 MV FFF	4.5	4.5	4.5	3.4	3.9	4.3
	NFS=10x10 mm^2					
6 MV FFF	10.5	10.5	10.0	8.4	9.5	9.0
10 MV FFF	9.5	9.9	10.0	9.5	10.0	9.5
	NFS=20x20 mm^2					
6 MV FFF	20.0	19.0	21.0	19.0	19.9	19.3
10 MV FFF	20.0	19.0	20.0	19.0	20.2	18.6

Table 7b Effective Field size (field width: max. slope)

	FS_{eff} [mm]						
	Exradin A26	IBA SFD	PTW 60012	Average/3(1)	SD	Average/2(2)	SD
	NFS = 5 x 5 mm^2						
6 MV FFF	5.20	4.46	4.20	4.62	0.52	4.33	0.18
10 MV FFF	4.50	3.91	4.10	4.17	0.30	4.00	0.13
	NFS = 10 x 10 mm^2						
6 MV FFF	10.50	9.17	9.25	9.64	0.75	9.21	0.06
10 MV FFF	9.70	9.75	9.75	9.73	0.03	9.75	0.00
	NFS = 20 x 20 mm^2						
6 MV FFF	19.49	19.97	19.60	19.69	0.25	19.79	0.27
10 MV FFF	19.49	19.49	19.38	19.46	0.06	19.44	0.08

(1) Average of FS_{eff} determined by the three detectors and (2) by the two diodes

The average differences in FS_{eff} (field width at 50% vs. maximum slope) [mm], when taking into account the scans measured with the two diodes (including the two FFF beam energies) are: 1.40 mm for the 5 x 5 mm^2; 0.64 mm for the 10 x 10 mm^2 and 0.48 mm for the 20 x 20 mm^2 field.

Figure 6 summarizes the results of the differences in effective field size for three detectors employed, i.e. two diodes and the Exradin A26 chamber and the two different approaches offered by OmniPro Accept to determine radiological field size.

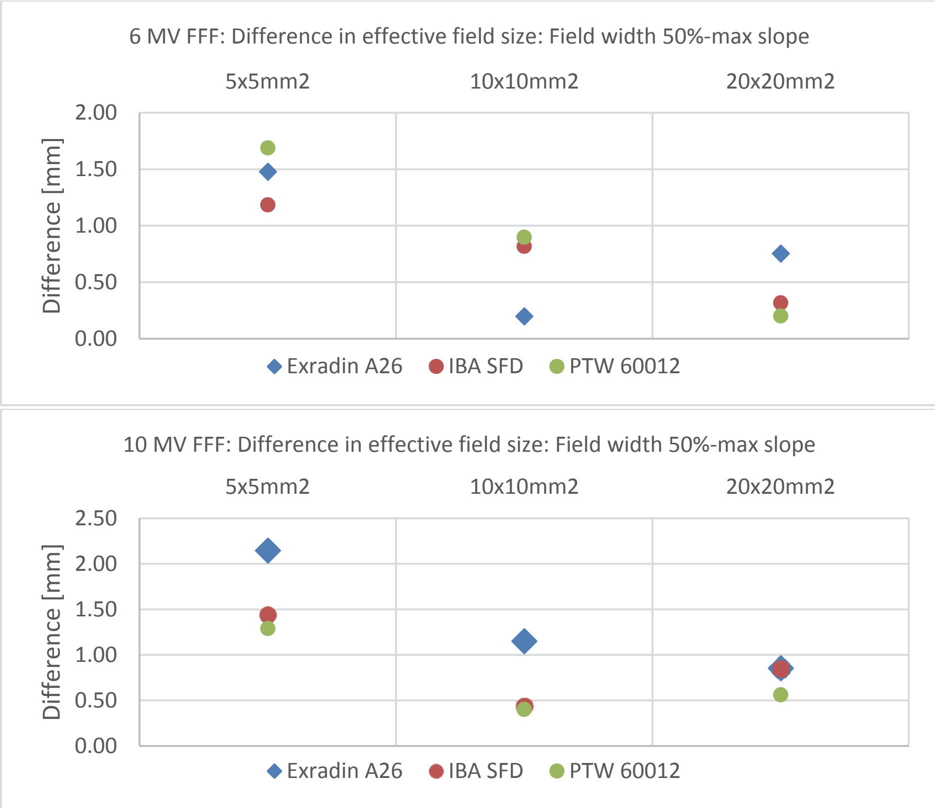

Figure 6 Field size difference: (field width at 50%-maximum slope).

Table 8 Comparison of field size distinguishing between the two different definitions of film measurements

	FS_{eff}: Difference with Film measurements [mm]					
	Field width 50%					
	6 MV FFF			10 MV FFF		
	5 x 5 mm^2	10 x 10 mm^2	20 x 20 mm^2	5 x 5 mm^2	10 x 10 mm^2	20 x 20 mm^2
Exradin A26	1.00	0.52	0.35	0.98	0.81	0.40
IBA SFD	-0.03	-0.20	0.40	-0.31	0.15	0.00
PTW 60012	0.22	-0.04	-0.10	-0.28	0.11	0.11
	Max slope					
	6 MV FFF			10 MV FFF		
	5 x 5 mm^2	10 x 10 mm^2	20 x 20 mm^2	5 x 5 mm^2	10 x 10 mm^2	20 x 20 mm^2
Exradin A26	-0.47	0.32	-0.40	-1.17	-0.34	-0.45
IBA SFD	-1.21	-1.02	0.08	-1.76	-0.29	-0.45
PTW 60012	-1.47	-0.94	-0.30	-1.57	-0.29	-0.56

Error! Reference source not found. shows the difference in FS_{eff} for FFF beams. On average, field sizes calculated from inline and crossline profiles using OmniPro Accept field width at 50% are larger than when using film profiles analysed with OmniPro IMRT (field width at 50%). The average difference (for all fields, all detectors and both FFF beams) is 0.23 mm (with average SD of 0.45). When the data for the Exradin A26 detector are not included in the analysis; the average difference is 0 mm and the average SD reduces to 0.04. The opposite happens when the field sizes are calculated using the maximum slope definition from OmniPro Accept. In this case, the average difference against film measurements is -0.68 mm, average SD = 0.13 (all fields, all detectors and both FFF beams). If the data from the Exradin A26 detector are not included, the difference increases to -0.81 mm (with average SD of 0.07)

An excel sheet with the details of the measurements and the analysis can be found in: Field size analysis.xlsx.

3.3 DETERMINATION OPF CLR WITH EXRADIN W1 SCINTILLATOR DETECTOR

CLR values are necessary for the determination of the OPF with the Exradin W1 detector. The robustness of the Underwood approach [4], in relation to the influence of the "test field" used for the CLR calculations and subsequently in the OPF determination, were assessed by performing measurements in both 4 x 4 and 5 x 5 cm^2 field sizes. **Table 9** presents the values of dose measured with the PTW semiflex chamber in order to allow for the CLR determination (Equation 3). **Table 10** summarises the results of the measurements and the calculated CLRs for all the energies used.

Table 9 IC measurements for CLR determination

	PTW 31010		
	Dose cGy		
	Ref 10 x 10 cm^2	Test 1 4 x 4 cm^2	Test 2 5 x 5 cm^2
6MV	84.81	74.56	76.82
10 MV	88.17	78.90	81.24
6 MV FFF	84.22	76.16	78.09
10 MV FFF	86.00	79.58	81.34

Table 10 Exradin W1 CLR values

	10 x 10 cm^2 (ref)		4 x 4 cm^2 (test)		5 x 5 cm^2 (test)		CLR (4 x 4 cm^2)	CLR (5 x 5 cm^2)
	SC1	SC2	SC1	SC2	SC1	SC2		
6 MV	62.697	58.727	52.920	48.107	55.137	50.487	0.625	0.611
6 MV FFF	58.470	53.070	50.053	43.557	52.067	45.810	0.636	0.633
10 MV	69.177	67.163	57.497	53.377	60.030	56.307	0.656	0.665
10 MV FFF	67.25	65.513	59.067	55.77	57.377	52.357	0.652	0.649

A detailed document with all the information and measurements to determine CLR with the scintillator can be found in: CLR Calculation (CLR sheet)

3.4 OUTPUT FACTORS

3.4.1 Field sizes from 4 x 4 cm^2 to 40 x 40 cm^2

Table 11 presents the results of the OPF from 4 x 4 cm^2 to 40 x 40 cm^2 field size for NPL Linac B (Beryl). Only the measurements with the PTW semiflex chamber are included in the table.

Table 11 Summary of OPF (4 x 4 cm^2 to 40 x 40 cm^2)

	6 MV	10 MV	6 FFF	10 FFF
Field Size [cm^2]	OPF			
4 x 4	0.879	0.895	0.904	0.925
5 x 5	0.906	0.921	0.927	0.946
6 x 6	0.930	0.940	0.946	0.961
7 x 7	0.950	0.958	0.962	0.973
8x8	0.969	0.974	0.977	0.983
9 x 9	0.985	0.988	0.989	0.993
10 x 10	1.000	1.000	1.000	1.000
12 x 12	1.023	1.022	1.018	1.011
15 x 15	1.053	1.047	1.038	1.026
20 x 20	1.090	1.076	1.062	1.040
25 x 25	1.117	1.095	1.077	1.049
30 x 30	1.135	1.108	1.086	1.055
40 x 30	1.142	1.111	1.089	1.056
35 x 35	1.149	1.118	1.092	1.058
40 x 40	1.153	1.119	1.093	1.059

The analysis of the OPF values for field sizes, ranging from 4 x 4 cm^2 to 40 x 40 cm^2, demonstrated that the average percentage difference ($1-OPF_{semiflex}/OPF_{CC13}$) between OPFs measured with the PTW semiflex and IBA CC13 chamber was 0.1%. The maximum difference was found to be 0.30% for 10 MV FFF, 30 x 40 cm^2 rectangular field. The percentage difference, defined as $1-OPF_{detector}/OPF_{average}$ (where $OPF_{average}$ is the result averaged over PTW Farmer, IBA CC13 and PTW Semiflex chamber), was found to be the highest for the 4 x 4 cm^2 field measured with the Farmer Chamber. The largest of all is 0.79 for 10 MV FFF. This effect was expected as Farmer chamber has significantly larger sensitive volume with respect to the other chambers used (see **Figure 7**).

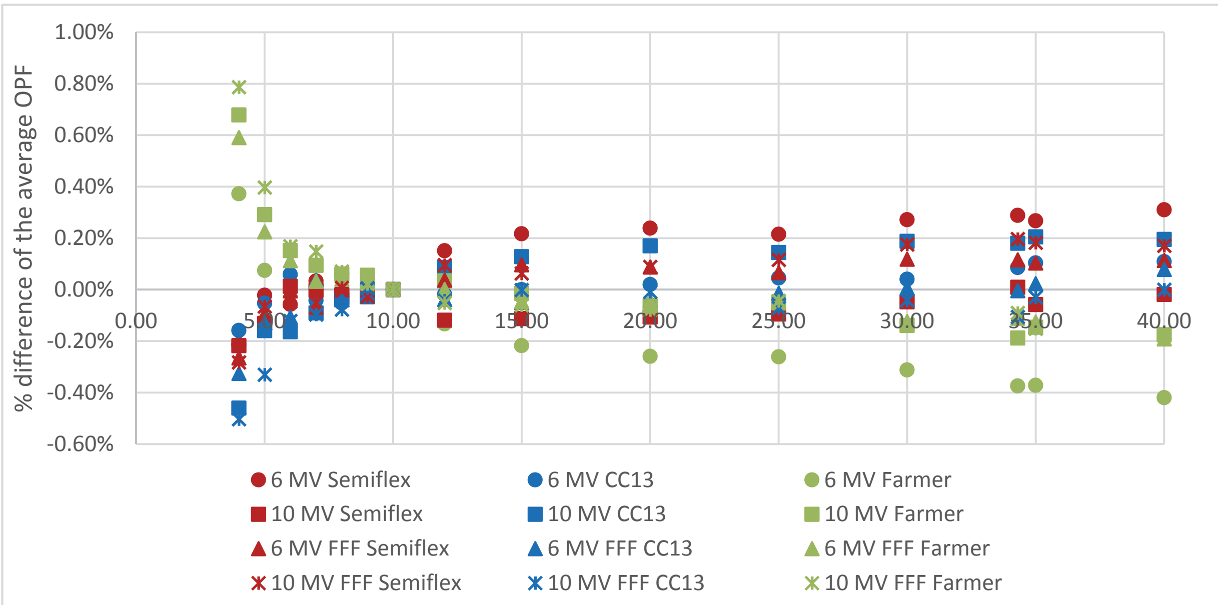

Figure 7 All Energies: % difference from the average OPF as determined with 3 different ionization chambers

It was an objective of this report to record measurements of the OPF with different detectors in order to gather data that could be used during the PCRD course and also to demonstrate the range of availability of different detectors in relation to the field size.

Whenever possible and for that range of field sizes, it is recommended to use an ionization chamber of smaller volume like the IBA CC13 or the PTW 31010 (semiflex).

It is important to note that the results include any variations in the reproducibility of the positioning of each detector for the given set of measurements.

3.4.2 Small Fields OPF

3.4.2.1 EBT-XD Films

Following the procedure explained in section 2.4.4, calibration curves for all the energies were created in Verisoft and OmniPro IMRT and packages (**Figure 8** and **Figure 9**, respectively).

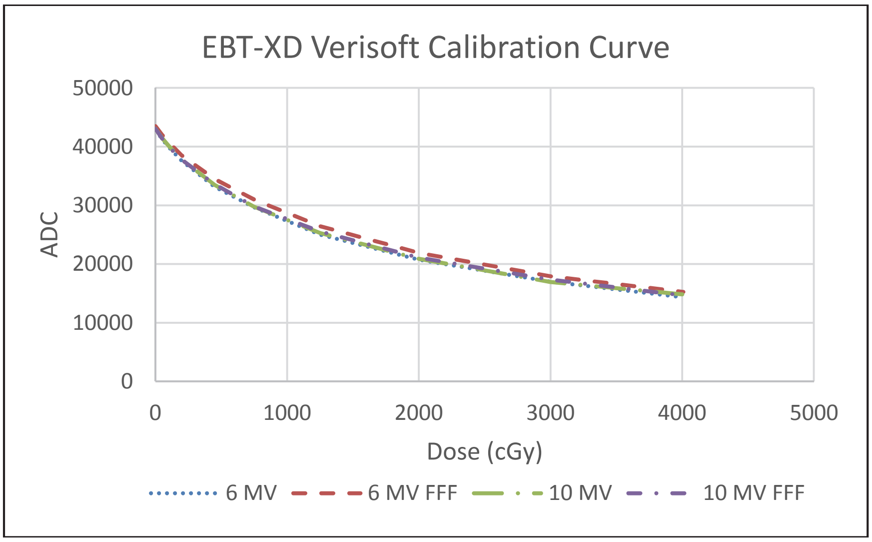

Figure 8 EBT-XD films calibration curve with PTW Verisoft.

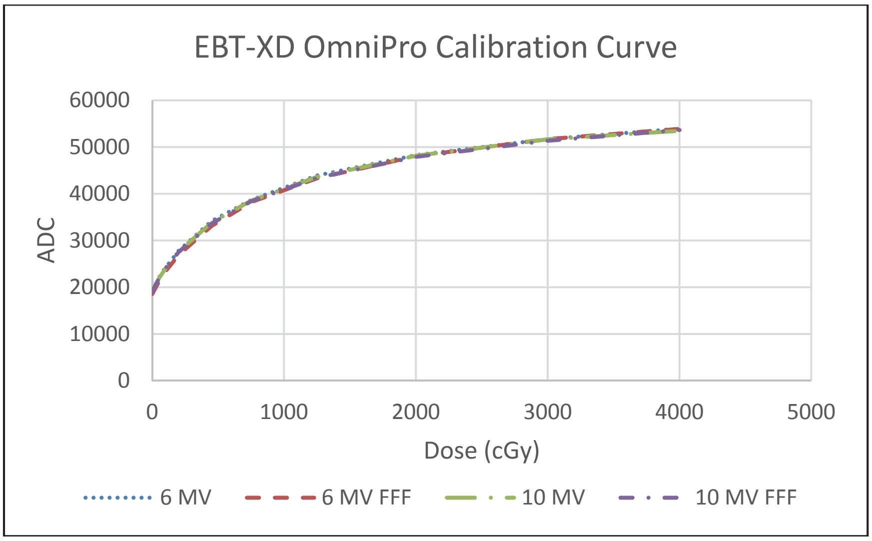

Figure 9 EBT-XD films calibration curve with IBA OmniPro-IMRT.

Tables 12 and 13 show OPF measured with EBT-XD films. They also show the difference in the OPF calculations by using two different applications for film dosimetry: OmniPro IMRT and Verisoft.

Table 12. OPF with EBT-XD films (6 MV and 6 MV FFF)

Equivalent Square [cm]	6 MV			6 MV FFF		
	OmniPro	Verisoft	Omn/Ver	OmniPro	Verisoft	Omn/Ver
0.5	0.472	0.468	-0.67%	0.494	0.502	1.51%
1	0.672	0.672	0.01%	0.685	0.670	-2.23%
2	0.794	0.784	-1.32%	0.822	0.820	-0.30%
3	0.845	0.847	0.21%	0.875	0.889	1.55%
4	0.864	0.867	0.33%	0.894	0.903	1.04%

Table 13. OPF with EBT-XD films (10 MV and 10 MV FFF)

Equivalent Square [cm]	10 MV			10 MV FFF		
	OmniPro	Verisoft	Omn/Ver	OmniPro	Verisoft	Omn/Ver
0.5	0.446	0.435	-2.42%	0.474	0.472	-0.52%
1	0.636	0.643	1.05%	0.658	0.647	-1.71%
2	0.799	0.813	1.67%	0.807	0.803	-0.50%
3	0.840	0.852	1.42%	0.876	0.881	0.63%
4	0.891	0.902	1.25%	0.909	0.920	1.25%

Although there are differences in the workflow for film dosimetry carried out with both applications, the results show generally good agreement for the OPF determination. For the 10 MV 0.5 x 0.5 cm^2 field and the 6 MV FFF 1 x 1 cm^2 field the differences between the OmniPro IMRT and Verisoft are -2.42% and -2.23%, respectively. For the rest of field sizes and energies the differences are smaller than 2% (the difference is well inside the overall uncertainty for measurements with EBT films using our current processing and analysis protocol).

3.4.2.2 Exradin W1 plastic scintillator detector

Using equation 2 (given in 2.3.1) and the CLR values presented in **Table 10**, measurements of channel 1 (CH1) and channel 2 (CH2) (see **Table 14**) for different field size were converted to a relative measure of dose (**Table 15**).

Table 14 Scintillator Chanel 1 & 2 measurements

	0.5 x 0.5 cm^2		1 x 1 cm^2		2 x 2 cm^2		3 x 3 cm^2		4 x 4 cm^2		5 x 5 cm^2		10 x 10 cm^2	
	SC1	SC2	SC1	SC2	SC1	SC2	SC1	SC2	SC1	SC2	SC1	SC2	SC1	SC2
6 MV	23.43	18.15	34.81	27.95	43.85	37.11	49.93	44.69	52.92	48.11	55.14	50.49	62.70	58.73
10 MV	24.29	19.57	36.47	30.51	47.46	41.58	53.97	49.31	57.50	53.38	60.03	56.31	69.18	67.16
6 FFF	25.14	19.69	36.18	29.40	44.30	37.37	47.68	40.94	50.05	43.56	52.07	45.81	58.47	53.07
10 FFF	24.78	19.59	36.96	30.73	47.73	41.56	52.44	46.64	59.07	55.77	57.38	52.36	67.25	65.51

Table 15 Relative dose (Exradin W1 detector)

		0.5 x 0.5 cm^2	1 x 1 cm^2	2 x 2 cm^2	3 x 3 cm^2	4 x 4 cm^2	5 x 5 cm^2	10 x 10 cm^2
6 MV	CLR 4x4	12.090	17.347	20.662	22.003	22.858	23.588	25.998
	CLR 5x5	12.339	17.731	21.171	22.616	23.518	24.280	26.804
10 MV	CLR 4x4	11.458	16.468	20.197	21.649	22.506	23.119	25.149
	CLR 5x5	11.274	16.182	19.807	21.186	22.006	22.591	24.519
6 FFF	CLR 4x4	12.611	17.468	20.516	21.622	22.335	22.915	24.698
	CLR 5x5	12.687	17.581	20.660	21.780	22.503	23.092	24.903
10 FFF	CLR 4x4	12.015	16.931	20.639	22.045	22.718	23.252	24.550
	CLR 5x5	12.079	17.031	20.774	22.196	22.899	23.422	24.763

Tables 16 and 17 show the results for OPF calculated using CLR values based on the 4 x 4 cm^2 and 5 x 5 cm^2 fields. The difference between the two approaches is also calculated.

Table 16. OPF: CLR from 4 x 4 cm^2 and 5 x 5 cm^2 fields

Field Size [cm^2]	OPF (CLR calculated with 4 x 4 cm^2 test field)				OPF (CLR calculated with 5 x 5 cm^2 test field)			
	6 MV	10 MV	6 MV FFF	10 MV FFF	6 MV	10 MV	6 MV FFF	10 MV FFF
0.5 x 0.5	0.465	0.456	0.511	0.489	0.460	0.460	0.509	0.488
1 x 1	0.667	0.655	0.707	0.690	0.661	0.660	0.706	0.688
2 x 2	0.795	0.803	0.831	0.841	0.790	0.808	0.830	0.839
3 x 3	0.846	0.861	0.875	0.898	0.844	0.864	0.875	0.896
4 x 4	0.879	0.895	0.904	0.925	0.877	0.898	0.904	0.925
5 x 5	0.907	0.919	0.928	0.947	0.906	0.921	0.927	0.946

Table 17. Difference in OPF in relation with the CLR calculation

Field Size [cm^2]	OPF: Difference using CLR with 4 x 4 cm^2 and 5 x 5 cm^2 fields			
	6 MV	10 MV	6 MV FFF	10 MV FFF
0.5 x 0.5	-1.02%	0.92%	-0.23%	-0.34%
1 x 1	-0.87%	0.78%	-0.18%	-0.28%
2 x 2	-0.62%	0.59%	-0.13%	-0.21%
3 x 3	-0.30%	0.38%	-0.10%	-0.18%
4 x 4	-0.21%	0.29%	-0.08%	-0.07%
5 x 5	-0.16%	0.23%	-0.06%	-0.13%

The results of output factor measurements are consistent when comparing the two sets of OPF based on CLR calculated from two different test fields (4 x 4 cm^2 and 5 x 5 cm^2). In the OPF measurements for the small fields, the largest difference between the W1 detector CLR value (calculated with Equation 3) for test fields of 4 x 4 cm^2 and 5 x 5 cm^2 (CLR_{4x4}-CLR_{5x5}), was found to be 0.014 for 6 MV. When comparing the two sets of OPFs for all field sizes (calculated with CLR_{4x4} or CLR_{5x5}), the resulting average percentage differences (1-OPF_{CLR4x4}/ OPF_{CLR5x5}) were -0.53%, -0.53%, -0.13% and -0.20% for 6 MV, 10 MV, 6 MV FFF and 10 MV FFF respectively. The largest difference was 1.02% for 6 MV for field size of 0.5 x 0.5 cm^2.

These results could be considered as a validation to the way we implemented the approach proposed by Underwood *el al.* [4]. The paper explains the possibilities to perform in-water measurements with the W1 plastic scintillator, and its stem axis parallel to the beam. The approach allows for the determination of CLR values by combining scintillator measurements from two field sizes (reference and a test) with a well established ion chamber (PTW 31010 Semiflex) measured doses.

3.4.2.3 Exradin A26 and Diodes' measurements. Daisy chain.

Results of OPF measurements with the Exradin A26 micro ionization chamber, the unshielded PTW E 60012 diode and the IBA SFD for field sizes from 0.5 x 0.5 cm^2 to 4 x 4 cm^2 are presented in **Table 18**.

Table 18 OPF for small fields.

Field Size [cm^2]	Exradin A26	PTW E Diode 60012 DC (1)	PTW E Diode 60012 NDC (2)	DC CF (3)	IBA SFD DC	IBA SFD NDC	DC CF
	6 MV						
0.5 x 0.5	0.411	0.496	0.488		0.492	0.479	
1 x 1	0.669	0.696	0.685		0.693	0.675	
2 x 2	0.801	0.800	0.787	1.017	0.798	0.778	1.027
3 x 3	0.846	0.843	0.829		0.843	0.821	
4 x 4	0.878	0.878	0.864		0.878	0.855	
	10 MV						
Field Size [cm^2]	Exradin A26	PTW E Diode 60012 DC	PTW E Diode 60012 NDC	DC CF	IBA SFD DC	IBA SFD NDC	DC CF
0.5 x 0.5	0.388	0.482	0.476		0.465	0.456	
1 x 1	0.636	0.672	0.663		0.673	0.660	
2 x 2	0.806	0.811	0.799	1.014	0.809	0.792	1.104
3 x 3	0.864	0.863	0.852		0.866	0.848	
4 x 4	0.899	0.899	0.886		0.899	0.880	
	6 MV FFF						
Field Size [cm^2]	Exradin A26	PTW E Diode 60012 DC	PTW E Diode 60012 NDC	DC CF	IBA SFD DC	IBA SFD NDC	DC CF
0.5 x 0.5	0.429	0.518	0.508		0.507	0.494	
1 x 1	0.692	0.717	0.704		0.708	0.691	
2 x 2	0.831	0.830	0.814	1.019	0.828	0.807	1.025
3 x 3	0.886	0.873	0.857		0.872	0.851	
4 x 4	0.904	0.904	0.888		0.904	0.882	
	10 MV FFF						
Field Size [cm^2]	Exradin A26	PTW E Diode 60012 DC	PTW E Diode 60012 NDC	DC CF	IBA SFD DC	IBA SFD NDC	DC CF
0.5 x 0.5	0.414	0.495	0.488		0.525	0.517	
1 x 1	0.669	0.697	0.688		0.708	0.697	
2 x 2	0.836	0.841	0.830	1.013	0.839	0.825	1.017
3 x 3	0.894	0.895	0.884		0.894	0.880	
4 x 4	0.925	0.925	0.913		0.925	0.910	

(1) DC stands for Daisy Chain corrected OPF, (2) NDC stands for non-Daisy Chain corrected OPF (direct ratio of the readings with the 10x10 cm^2 field), (3) CF is the Daisy Chain correction factor

As explained in section 2.4.3, in order to correct for the over-response of silicon detectors to field-size dependent changes in the low-energy component of the photon spectrum due to secondary scatter products, the Daisy Chain approach was used to calculate OPF based on measurements with the diodes. The Exradin A26 chamber was used as the class detector and the 4 x 4 cm^2 was the intermediate (connecting) field.

$$CF_{diode} = \frac{M_{diode}(10x10cm^2)}{M_{diode}(4x4cm^2)} \times \frac{M_{A26}(4x4cm^2)}{M_{A26}(10x10cm^2)} \quad (8)$$

Figure 10 shows the difference in detector response in relation to average OPF. As expected, the larger difference between individual detectors is for the 0.5 x 0.5 cm^2 field. The graph illustrates that with the Exradin A26 IC, the volume averaging effect is present for the smaller fields. In the case of both diodes, the perturbation produced by the high density of the material of the detectors in comparison with that of water, is the dominant effect, given the smaller dimensions of these two detectors. (see **Table 1**)

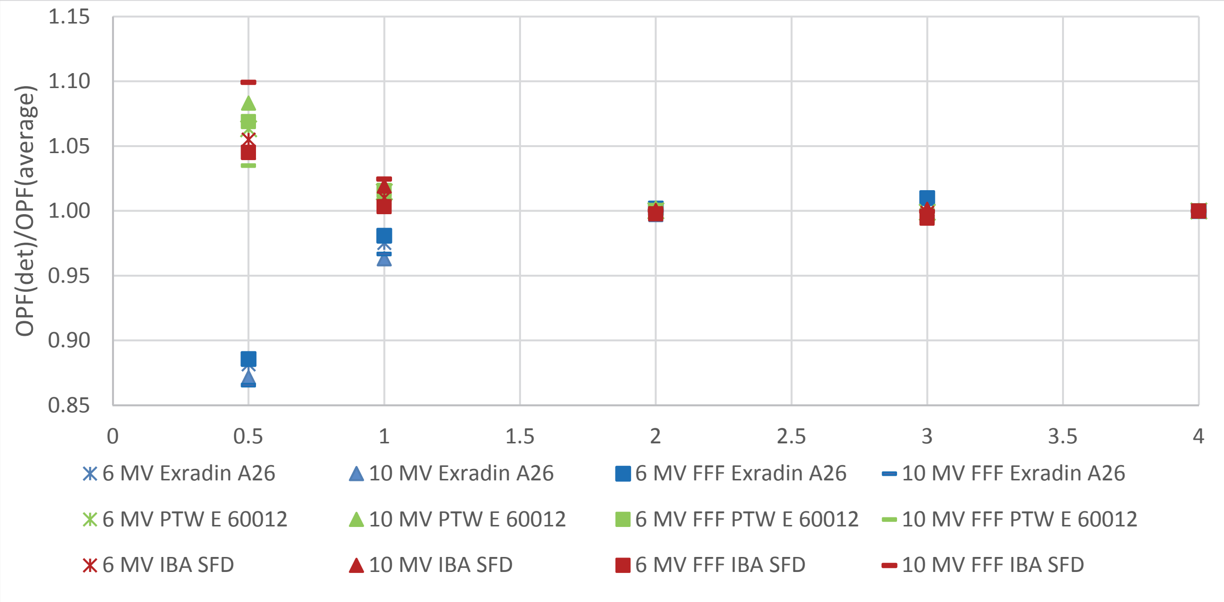

Figure 10 Difference in detector response in relation to the average OPF.

3.4.2.4 Multi detector comparison

The following set of tables present a multi detector comparison against the measurements with the Exradin W1 plastic scintillator.

Table 19 a and b. Multi detector comparison with Exradin W1 plastic scintillator (6 MV and 10 MV).

	6 MV						
Field Size [cm^2]	Exradin A26	PTW E Diode 60012	PTW E Diode 60012 NDC	IBA SFD	IBA SFD NDC	W1	Film
0.5 x 0.5	0.411	0.496	0.488	0.492	0.479	0.465	0.472
1 x 1	0.669	0.696	0.685	0.693	0.675	0.667	0.672
2 x 2	0.801	0.800	0.787	0.798	0.778	0.795	0.794
3 x 3	0.846	0.843	0.829	0.843	0.821	0.846	0.845
4 x 4	0.878	0.878	0.864	0.878	0.855	0.879	0.864
	Difference vs. W1 (1)						
0.5 x 0.5		-6.58%	-4.84%	-5.75%	-2.98%		-1.41%
1 x 1	-0.29%	-4.34%	-2.63%	-3.87%	-1.15%		-0.65%
2 x 2	-0.79%	-0.63%	1.01%	-0.46%	2.16%		0.06%
3 x 3	0.03%	0.38%	2.01%	0.42%	3.03%		0.14%
4 x 4	0.13%	0.13%	1.76%	0.13%	2.74%		1.70%

(1) Difference vs W1 = $1-(OPF_{detector}/OPF_{W1})$[%]

Field Size [cm^2]	10 MV						
	Exradin A26	PTW E Diode 60012	PTW E Diode 60012 NDC	IBA SFD	IBA SFD NDC	W1	Film
0.5 x 0.5	0.388	0.482	0.476	0.465	0.456	0.456	0.446
1 x 1	0.636	0.672	0.663	0.673	0.660	0.655	0.636
2 x 2	0.806	0.811	0.799	0.809	0.792	0.803	0.799
3 x 3	0.864	0.863	0.852	0.866	0.848	0.861	0.840
4 x 4	0.899	0.899	0.886	0.899	0.880	0.895	0.891
	Difference vs W1 (1)						
0.5 x 0.5		-5.86%	-4.42%	-2.13%	-0.04%		2.17%
1 x 1	2.85%	-2.64%	-1.25%	-2.82%	-0.71%		2.90%
2 x 2	-0.40%	-0.92%	0.45%	-0.74%	1.33%		0.46%
3 x 3	-0.42%	-0.28%	1.08%	-0.54%	1.52%		2.45%
4 x 4	-0.40%	-0.40%	0.96%	-0.40%	1.65%		0.49%

Table 20 a. and b. Multi detector comparison with Exradin W1 plastic scintillator (6 MV FFF and 10 MV FFF).

Field Size [cm^2]	6 MV FFF						
	Exradin A26	PTW E Diode 60012	PTW E Diode 60012 NDC	IBA SFD	IBA SFD NDC	W1	Film
0.5 x 0.5	0.429	0.518	0.508	0.507	0.494	0.511	0.494
1 x 1	0.692	0.717	0.704	0.708	0.691	0.707	0.685
2 x 2	0.831	0.830	0.814	0.828	0.807	0.831	0.822
3 x 3	0.886	0.873	0.857	0.872	0.851	0.875	0.875
4 x 4	0.904	0.904	0.888	0.904	0.882	0.904	0.894
	Difference vs W1 (1)						
0.5 x 0.5		-1.47%	0.42%	0.77%	3.21%		3.17%
1 x 1	2.10%	-1.38%	0.52%	-0.13%	2.33%		3.20%
2 x 2	-0.07%	0.08%	1.95%	0.35%	2.80%		0.98%
3 x 3	-1.21%	0.23%	2.09%	0.36%	2.81%		0.08%
4 x 4	-0.01%	-0.01%	1.86%	-0.01%	2.45%		1.17%

Field Size [cm^2]	10 MV FFF						
	Exradin A26	PTW E Diode 60012	PTW E Diode 60012 NDC	IBA SFD	IBA SFD NDC	W1	Film
0.5 x 0.5	0.414	0.495	0.488	0.525	0.517	0.489	0.474
1 x 1	0.669	0.697	0.688	0.708	0.697	0.690	0.658
2 x 2	0.836	0.841	0.830	0.839	0.825	0.841	0.807
3 x 3	0.894	0.895	0.884	0.894	0.880	0.898	0.876
4 x 4	0.925	0.925	0.913	0.925	0.910	0.925	0.909
	Difference vs W1 (1)						
0.5 x 0.5		-1.05%	0.29%	-7.33%	-5.54%		3.07%
1 x 1	3.06%	-1.11%	0.23%	-2.73%	-1.02%		4.58%
2 x 2	0.55%	-0.10%	1.23%	0.18%	1.84%		4.00%
3 x 3	0.43%	0.29%	1.60%	0.39%	2.05%		2.50%
4 x 4	0.01%	0.01%	1.33%	0.01%	1.68%		1.81%

In general, for all energies and field sizes used in this study, OPFs measured with films are smaller than those determined with the W1 detector. The average agreement of the OPF difference against W1 detector, when taking into account only 2 x 2, 3 x 3 and 4 x 4 cm^2 fields, for the four beam qualities of interest was 1.32%. That suggests that larger differences, such as the one observed for the smaller fields could be related to the fact that the W1 although being considered a water equivalent detector, and with a diameter similar to the PTW E 60012 diode, has a larger sensitive volume than the two diodes used in this study **(see Table 1**). It is necessary to note that the results for 10 MV FFF show a larger difference between the film and the W1 detector-measured OPFs.

Applying the Daisy chain method improves the agreement between the OPF for the same given field size with the PTW E 60012 and the IBA SFD by reducing the average difference from 1.43% to 0.87%. These results demonstrate the need for applying the correction due to the variation of the effect of the silicon diodes under response to the low energy components of the spectrum in relation to the field size.

Figure 11 presents a comparison of OPF with different detectors for the 10 MV FFF beam.

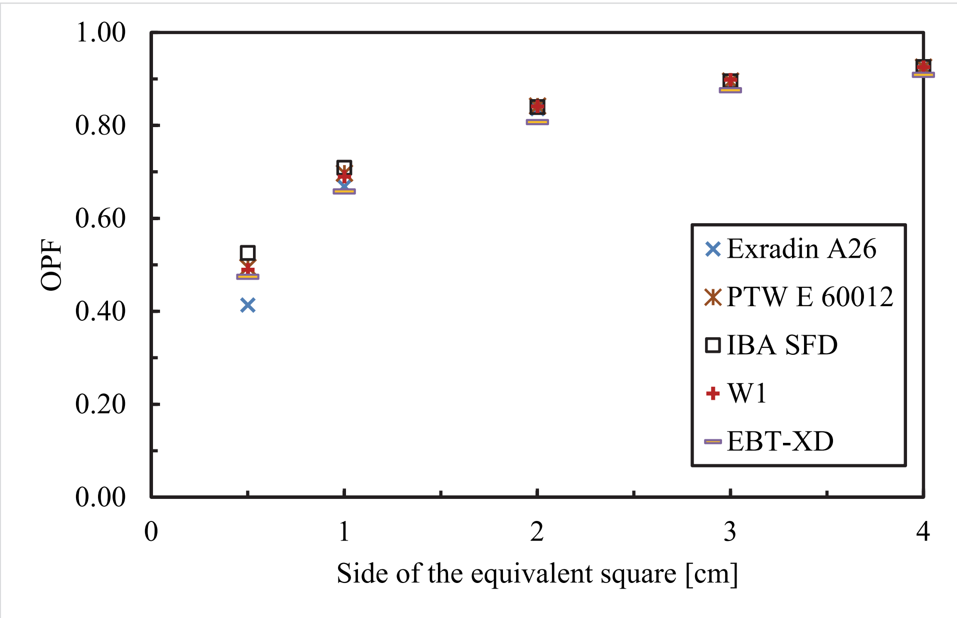

Figure 11 OPF 10 MV FFF, SSD 90 cm, depth 10cm (IBA SFD and PTE E 60012 diode have been determined using the daisy chain method

3.4.2.5 Clinical assessment of OPF variation according to the detector.

In order to assess the impact in dose calculations from using different OPF for small fields, a Pinnacle plan was created. The plan consisted of one 360^0 conformal arc with the isocentre in the centre of a ROI with a volume of 0.16 cm^3. The ROI simulated a brain metastasis and the STEEV phantom (CIRS) was used as the anatomy for dose calculations (**Figure 12)**. The dose was prescribed to be 2000 cGy to the 90% of the ROI mean (one fraction treatment). The equivalent square for such beam, as used by Pinnacle for MU Hand computation parameters, was 0.6 cm.

The plan was calculated for all the beams included in this study and with OPF for: Exradin W1, EBT XD film, PTW E 60012 (daisy chain method) and IBA SFD (daisy chain method) as part of the modelling parameters. A calculation was also performed for the 6 MV beam, with the OPF for the IBA SFD without applying the daisy chain method. That combination detector-beam quality showed the maximum difference in the OPF with and without using the daisy chain method (**Table 18**).

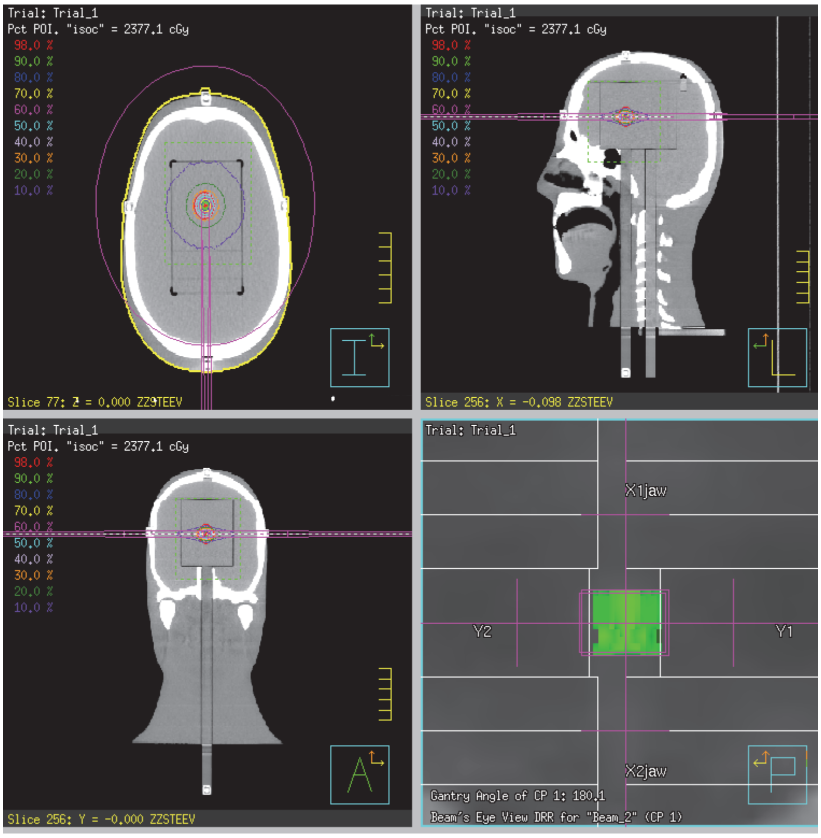

Figure 12 Pinnacle plan.

Using a calculation grid of 1.5 mm, no significant differences (less than 0.1%) in the dose to a point (isocentre) were detected.

Further investigation in relation to the effect of small fields OPF in Pinnacle calculations needs to be carried out. Optimization parameters and other constrains that apply to IMRT and VMAT inverse planning need to be assessed. That will required more complex plans to be created and calculated.

3.4.2.6 Experimental determination of detector, field size and measurement condition specific correction factors for small fields.

There is ample information about output factors for small fields. However, it has proven difficult to find published OPF for our measurements conditions (i.e. SSD of 90 cm and 10 cm depth), with an Elekta Versa linac (Agility MLC) and for beams other than 6 MV. Different ways of calculating or measuring corrections for detectors suitable for small fields can also be found in the literature. However, few results are available that could be used as practical guidance or that could be used to compare with our own measurements.

According to Alfonso *et al.* algorithms [13] and following the assumptions as per in Benmakhouf *et al.* [14], we experimentally determined correction factors $k^{f\,clin,fmsr}_{Qclin,Qmsr}$ that can be applied to the measured output factors (ratios of readings) in small fields:

$$\Omega^{fclin,fmsr}_{Qclin,Qmsr} = \frac{D^{f\,clin}_{w,Qclin}}{D^{f\,msr}_{w,Qmsr}} = \frac{M^{f\,clin}_{Q\,clin}}{M^{f\,msr}_{Q\,msr}} \left[\frac{D^{f\,clin}_{w,Qclin} / M^{f\,clin}_{Q\,clin}}{D^{f\,msr}_{w,Q\,msr} / M^{f\,msr}_{Q\,msr}} \right] \quad (8)$$

$$k_{Qclin,Qmsr}^{f\,clin,fmsr} = \left[\frac{D_{w,Qclin}^{f\,clin} / M_{Q\,clin}^{f\,clin}}{D_{w,Q\,msr}^{f\,msr} / M_{Q\,msr}^{f\,msr}}\right] \quad (9)$$

where:

$\Omega_{Qclin,Qmsr}^{fclin,fmsr}$ is a field factor that converts the absorbed dose to water for the machine-specific reference field f_{msr} to the absorbed dose to water for the clinical field f_{clin}.

$k_{Qclin,Qmsr}^{f\,clin,fmsr}$ is a correction factor which accounts for the difference between the detector response in the fields f_{clin} and f_{msr}

Our work is performed in a conventional linear accelerator. We can therefore assume f_{msr} (machine specific reference field) to be the reference 10 x 10 cm^2 field (f_{ref}). **Equation 9** can be rewritten as follow:

$$k_{Qclin,Qref}^{fclin,fref} = \left[\frac{D_{w,Qclin}^{fclin}}{D_{w,Qref}^{fref}}\right]_{W1\ or\ film} \times \left[\frac{M_{Qref}^{fref}}{M_{Qclin}^{fclin}}\right]_{det} \quad (10)$$

To experimentally determine correction factors to the measured OPF, it is necessary to quantify the dose at the reference point with detectors that are preferably water equivalent and with a small volume so that the volume averaging effect is negligible ($\left[\frac{D_{w,Qclin}^{fclin}}{D_{w,Qref}^{fref}}\right]$)

Two detectors in our studies complied with those conditions: the plastic scintillator W1 and the EBT-XD films. We were unable to reproduce Underwood *et al.* [4] results and validate the use of the W1 detector with dose measurements performed with the EBT XD film measurements of dose (average difference of the OPF measured with both detectors 1.8%, larger than 3% for 10 MV FFF). We are justifying it by the fact that there are uncertainties in our dose calculations with the films without using the triple channel dosimetry algorithm. Those uncertainties are dose dependent and the dose at the reference point for a 10 x 10 cm^2 field can be twice as high as the one for 0.5 x 0.5 cm^2 field. EBT-XD films are relatively new on the market. The time frame for this project did not allow us to establish the magnitude of the errors introduced in dose calculations when these types of films are analysed with tools that only use the red channel.

We directly calculated $k_{Qclin,Qref}^{fclin,fref}$ from dose (relative) measurements with the Exradin W1 detector and repeated the process with the dose measured with the EBT XD films. Then the results were compared.

Figure 13 and Figure 14 show the field-detector-beam quality specific factors for all the possible combinations. The results are normalized to the 4 x 4 cm^2 field. The results confirm the different behaviour of the Exradin A26 IC in comparison with the diode detectors and the fact that for the 0.5 x 0.5 cm^2 field, it is completely unacceptable to use that particular detector for OPF determination.

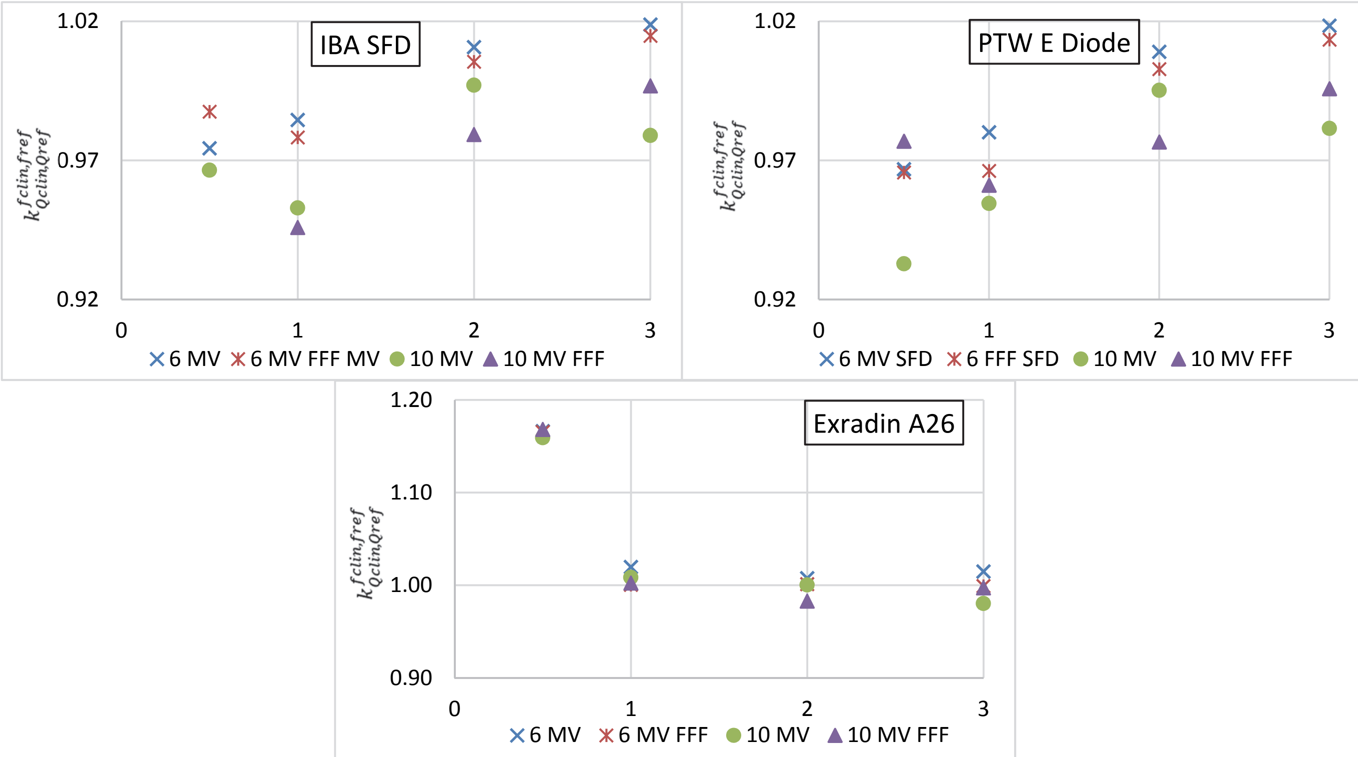

Figure 13. $k_{Qclin,Qref}^{fclin,fref}$ **correction factors as function of the nominal field size. Calculation based on measurements with EBT-XD films. Factors normalized to the 4 x 4 cm² field.**

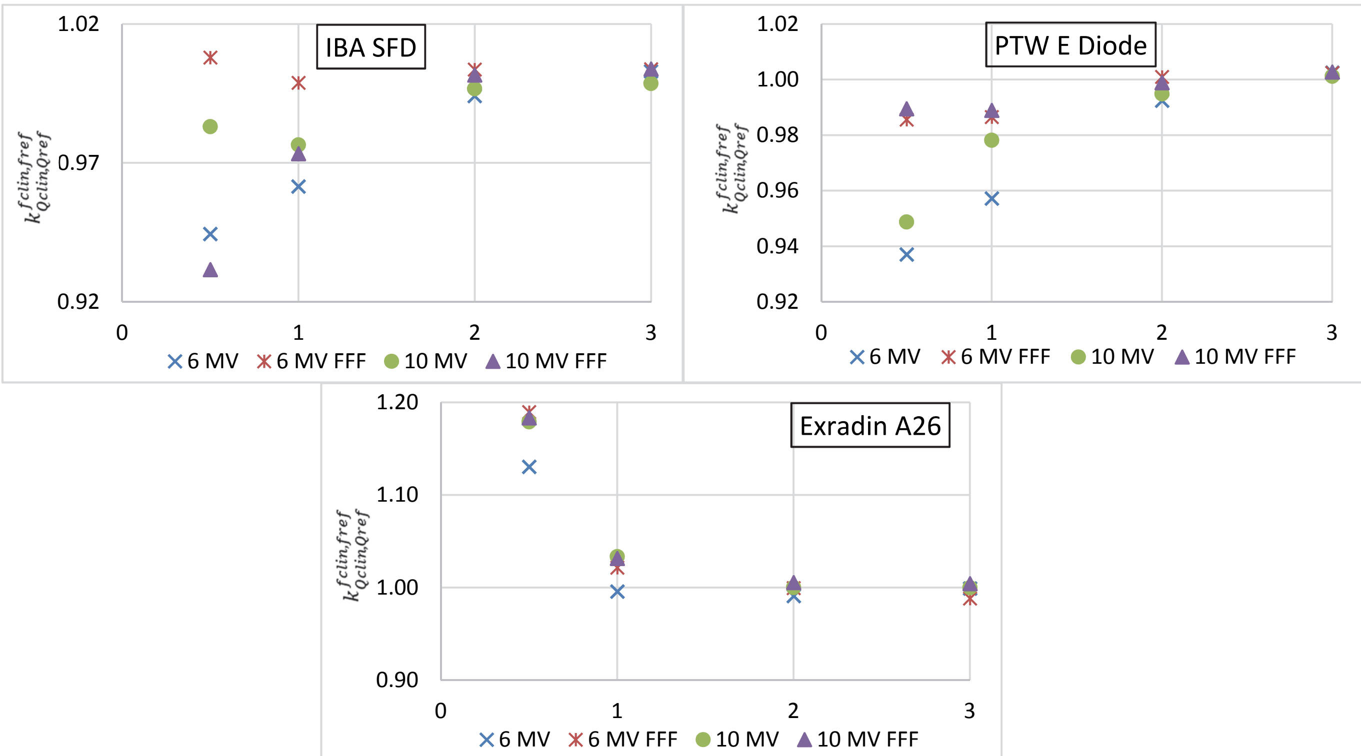

Figure 14. $k_{Qclin,Qref}^{fclin,fref}$ **correction factors as function of the nominal field size. Calculation based on measurements with Exradin W1 scintillator. Factors normalized to the 4 x 4 cm² field.**

A comparison between the OPF calculated by using the daisy chain method or by applying the detector and field size specific correction factor is presented in tables 21, 22 and 23.

Table 21. OPF calculated using the $k_{Qclin,Qref}^{fclin,\,fref}$ correction factor (PTW E Diode).

Field size [cm²]	PTW E Diode											
	6 MV			10 MV			6 MV FFF			10 MV FFF		
	OPF (DC)	$\Omega_{Qclin,Qref}^{fclin,\,fref}$	% Diff.	OPF (DC)	$\Omega_{Qclin,Qref}^{fclin,\,fref}$	% Diff.	OPF (DC)	$\Omega_{Qclin,Qref}^{fclin,\,fref}$	% Diff.	OPF (DC)	$\Omega_{Qclin,Qref}^{fclin,\,fref}$	% Diff.
0.5 x 0.5	0.496	0.465	6.24%	0.482	0.456	5.48%	0.518	0.511	1.43%	0.495	0.489	1.13%
1.0 x 1.0	0.696	0.667	4.13%	0.672	0.655	2.55%	0.717	0.707	1.36%	0.697	0.690	1.05%
2.0 x 2.0	0.800	0.795	0.66%	0.811	0.803	0.97%	0.83	0.831	-0.08%	0.841	0.841	0.04%
3.0 x 3.0	0.843	0.846	-0.40%	0.863	0.861	0.25%	0.873	0.875	-0.28%	0.895	0.898	-0.33%
4.0 x 4.0	0.878	0.879	-0.14%	0.899	0.895	0.45%	0.904	0.904	-0.04%	0.925	0.925	-0.04%

Table 22. OPF calculated using the $k_{Qclin,Qref}^{fclin,\,fref}$ correction factor (IBA SFD).

Field size [cm²]	PTW E Diode											
	6 MV			10 MV			6 MV FFF			10 MV FFF		
	OPF (DC)	$\Omega_{Qclin,Qref}^{fclin,\,fref}$	% Diff.	OPF (DC)	$\Omega_{Qclin,Qref}^{fclin,\,fref}$	% Diff.	OPF (DC)	$\Omega_{Qclin,Qref}^{fclin,\,fref}$	% Diff.	OPF (DC)	$\Omega_{Qclin,Qref}^{fclin,\,fref}$	% Diff.
0.5 x 0.5	0.492	0.465	5.44%	0.465	0.456	2.09%	0.481	0.485	-0.74%	0.525	0.489	6.78%
1.0 x 1.0	0.693	0.667	3.73%	0.673	0.655	2.74%	0.708	0.708	0.07%	0.708	0.690	2.59%
2.0 x 2.0	0.798	0.795	0.46%	0.809	0.803	0.73%	0.828	0.830	-0.27%	0.839	0.841	-0.20%
3.0 x 3.0	0.843	0.846	-0.42%	0.866	0.861	0.54%	0.872	0.876	-0.41%	0.894	0.898	-0.44%
4.0 x 4.0	0.878	0.879	-0.13%	0.899	0.895	0.40%	0.904	0.904	-0.01%	0.925	0.925	-0.04%

Table 23. OPF calculated using the $k_{Qclin,Qref}^{fclin,\,fref}$ correction factor (Exradin A26).

Field size [cm²]	Exradin A26							
	6 MV		10 MV		6 MV FFF		10 MV FFF	
	OPF	$\Omega_{Qclin,Qref}^{fclin,\,fref}$	OPF	$\Omega_{Qclin,Qref}^{fclin,\,fref}$	OPF	$\Omega_{Qclin,Qref}^{fclin,\,fref}$	OPF	$\Omega_{Qclin,Qref}^{fclin,\,fref}$
0.5 x 0.5	0.411	0.465	0.388	0.456	0.429	0.511	0.414	0.489
1.0 x 1.0	0.669	0.667	0.636	0.655	0.692	0.707	0.669	0.690
2.0 x 2.0	0.801	0.795	0.806	0.803	0.831	0.831	0.836	0.841
3.0 x 3.0	0.846	0.846	0.864	0.861	0.886	0.875	0.894	0.898
4.0 x 4.0	0.878	0.879	0.899	0.895	0.904	0.904	0.925	0.925

3.4.2.7 OPF fields 0.5 x 0.5 cm² to 3 x 3 cm². Summary

The following tables summarize the OPF for the smaller field sizes of interest for this study.

Table 24. Summary. Small fields OPF.

Field size [cm²]	PTW E 60012 DC				PTW E 60012 $k_{Qclin,Qref}^{fclin,fref}$			
	6 MV	6 MV FFF	10 MV	10 MV FFF	6 MV	6 MV FFF	10 MV	10 MV FFF
0.5 x 0.5	0.496	0.518	0.451	0.495	0.465	0.511	0.456	0.489
1.0 x 1.0	0.696	0.717	0.672	0.697	0.667	0.707	0.655	0.690
2.0 x 2.0	0.800	0.830	0.811	0.841	0.795	0.831	0.803	0.841
3.0 x 3.0	0.843	0.873	0.863	0.895	0.846	0.875	0.861	0.898

Field size [cm^2]	IBA SFD DC				IBA SFD $k_{Qclin,Qref}^{fclin,fref}$			
	6 MV	6 MV FFF	10 MV	10 MV FFF	6 MV	6 MV FFF	10 MV	10 MV FFF
0.5 x 0.5	0.492	0.481	0.465	0.525	0.465	0.485	0.456	0.489
1.0 x 1.0	0.693	0.708	0.673	0.708	0.667	0.708	0.655	0.690
2.0 x 2.0	0.798	0.828	0.809	0.839	0.795	0.830	0.803	0.841
3.0 x 3.0	0.843	0.872	0.866	0.894	0.846	0.876	0.861	0.898

Field size [cm^2]	Exradin A26				Exradin A26 $k_{Qclin,Qref}^{fclin,fref}$			
	6 MV	6 MV FFF	10 MV	10 MV FFF	6 MV	6 MV FFF	10 MV	10 MV FFF
0.5 x 0.5	0.411	0.429	0.388	0.414	0.465	0.511	0.456	0.489
1.0 x 1.0	0.669	0.692	0.636	0.669	0.667	0.707	0.655	0.690
2.0 x 2.0	0.801	0.831	0.806	0.836	0.795	0.831	0.803	0.841
3.0 x 3.0	0.846	0.886	0.864	0.894	0.846	0.875	0.861	0.898

Calculating OPF for small fields by using the $k_{Qclin,Qref}^{fclin,fref}$ reduces the absolute average difference with in the PTW E 60012 and IBA SFD diodes from 1.32% to 0.34% (averaging over all the field sizes). When analysing the absolute average difference for the 0.5 x 0.5 cm^2 and 1 x 1 cm^2 fields, the OPF agreement improves from 2.61% to 0.67%.

3.4.2.8 Uncertainty budget for the $k_{Qclin,Qref}^{fclin,fref}$ determination

Following recommendations from Chung *et al.* [15], an uncertainty budget for the experimental determination of the small fields and detector specific correction factors based on measurements with the Exradin W1 detector was established (see **Table 25**).

Table 25 Uncertainty budget on the correction factor $k_{Qclin,Qref}^{fclin,fref}$ for PTW E 60012 and IBA SFD diodes based on Exradin W1 measurements of dose.

Source of uncertainty	Type A (%)	Type B (%)
Reference detector		
Reproducibility of W1 readings in the clinical field	0.03$^{(1)}$	
Reproducibility of W1 readings in the reference field	0.03$^{(2)}$	
Positioning of the detector	0.1	
CLR determination		0.9$^{(3)}$
Overall Relative dose determination for W1 (reference) detector	0.907	
Diode		
Reproducibility of IBA SFD readings in the clinical field	0.003	
Reproducibility of PTW E diode readings in the clinical field	0.018	
Reproducibility of IBA SFD readings in the reference field	0.001	
Reproducibility of IBA SFD readings in the reference field	0.003	
Positioning of the detector	0.1	
Overall Relative dose determination for field detectors	0.1-0.101	
Overall $k_{Qclin,Qref}^{fclin,fref}$	0.905	

(1) Based on the reproducibility of the measurements of CH1 and CH2 averaged over all field sizes and the 10 x 10 cm^2 field respectively

(2) Based on analysis of profiles measured with W1 for 0.5 x 0.5 cm^2 and the impact of 0.1 mm variation of the position on the relative dose

(3) CLR uncertainty based on the study by Carrasco *et al.* [17]

4 CONCLUSIONS

The report presents a set of reference beam quality index parameters: TPR20/10 and TPR10 for all the energies of interest for this study for NPL's linac B. It confirms that their determination is not significantly influenced by the size of the ionization chamber used for the measurements.

A set of output factors for field sizes from 4 x 4 cm^2 to 40 x 40 cm^2 measured with a PTW 31010 (semiflex) ionization chamber is presented. The results in **Table 11** could be used as a reference set of OPF for Pinnacle commissioning and also for annual QA for linac B. They could also be used as a reference to compare with sets of data acquired during the NPL commissioning service RD18 when working on similar linacs and with the same reference conditions as used in our TPS commissioning. For comparison purposes and to investigate the relation between the OPFs and the size of the detector (in particular for FFF beams), a set of OPF was also measured with the IBA CC13 and the PTW 30013 Farmer ionization chamber. The analysis of the results show that the larger size of the Farmer IC in the longitudinal axes makes it unsuitable for measurements of field sizes smaller than 5 x 5 cm^2.

A consistent CAX value (larger than 1 mm) for 6 MV FFF in the crossline direction was found in profiles measured with different detectors as required in this study. Although it is not relevant for this study, this is a finding that will be essential to address when comparison of measurements with Monte Carlo calculations will be performed. A fine-tuning of 1R could improve the CAX in relation with the rest of the analysed beams.

The Effective Field Size definition for small fields was introduced in our analysis. The impact in the determination of field sizes for FFF beams, as reported by two different analysis tools from OmniPro-Accept, was assessed. Field size and penumbra definition for FFF beams is still a subject of academic and clinical discussions

EBT-XD films were also used as detector (water equivalent and with suitable resolution for small fields). Calibration curves for EBT-XD films for all the energies demonstrated the energy independence of the films in the range of Beam Qualities (TPR20/10) between 0.683 (6 MV) and 0.735 (10 MV FFF). **Table 12** and **Table 13** demonstrated that using PTW Verisoft and IBA OmniPro IMRT analysis tools for calculation of OPF leads to results that can be considered equivalent. The characteristic of the films allowed for a measurement of dose for fields ranging from 0.5 x 0.5 cm^2 to 4 x 4 cm^2 plus for the 10 x 10 cm^2. Applying the Alfonso *et al.* formalism, the film was used as a class detector to establish specific detector and field size correction factors for the diodes used in this work and for the Exradin A26 IC.

The approach presented by Underwood *et al.* was the base for the measurements of dose and OPF with the Exradin W1 plastic scintillator detector. Similarly to the films, the W1 can be considered water equivalent although, in comparison with the diodes used in this study, it has a larger sensitive volume. The consistency of the approach by Underwood was proven by using two different fields size to determine the values of the CLR. As well as the films, the W1 detector was used as a class detector to establish specific detector and field size correction factors for the diodes used in this work and for the Exradin A26 IC. A measurement set of (relative) dose for fields from 0.5 x 0.5 cm^2 to 4 x 4 cm^2 and additionally for the 10 x 10 cm^2 was used for that purpose.

Exradin A26 IC is suitable for measurements of OPF down to 1 x 1 cm^2. For the smaller field, included in this study, the volume of air irradiated is unlikely to be uniform as the penumbra is part of the radiation field covering the chamber. There also exists an increase in the lateral electronic disequilibrium, resulting in lower dose deposition. Those effects result in an underestimation of the true dose, which consequently leads to smaller OPF than expected [16].

The Exradin A26 IC was selected as a class detector to apply the daisy chain method to dose measured with the IBA SFD and PTW E 60012 diodes in small fields. A set of OPF for fields 0.5 x 0.5 cm^2 to 3 x 3 cm^2 under those conditions is presented in **Table 18** OPF for small fields. These results can be used as reference for future measurements and also to compare with sets of data acquired during the NPL commissioning service RD18 when working in similar linacs and with the same reference conditions as we use for the TPS commissioning.

An analysis of the clinical impact of using different values of OPF (according to its calculation method: ratio of readings (NDC), daisy chain (DC), ratio of readings corrected by the factor $k_{Qclin,Qref}^{fclin,fref}$) was performed. A clinical plan based on 1 arc conformed to a ROI with a volume relevant to the field sizes of interest was calculated in Pinnacle for all the combinations of OPF and beam qualities models, i.e. 6 MV, 10 MV, 6 MV FFF and 10 MV FFF. No significant difference (>0.1%) for a point dose calculation (isocentre=centre of ROI) was found for any of the combinations.

A set of experimentally determined field size and detector specific correction factors was established. The comparison for the same experimental approach by using two different "reference" detectors: EBT films and Exradin W1 plastic scintillator was also reported. A set of OPF for fields from 0.5 x 0.5 cm^2 to 3 x 3 cm^2 calculated from the directly measured ratio of diodes readings, corrected by the specific correction factor $k_{Qclin,Qref}^{fclin,fref}$ is presented for the IBA SFD, the PTW E 60012 diodes and the Exradin A26 IC (**Table 24**).

Finally, an uncertainty budget analysis on the correction factor $k_{Qclin,Qref}^{fclin,fref}$ for PTW E 60012 and IBA SFD diodes based on Exradin W1 measurements of dose is also presented.

5 BIBLIOGRAPHY

[1] R. Alfonso, P. Andreo, R. Capote, M. S. Huq, W. Kilby, P. Kjall, T. R. Mackie, H. Palmans, K. Rosser, J. Seuntjens, W. Ullrich and S. Vatnitsky, "A new formalism for reference dosimetry of small and nonstandard fields," *Medical Physics,* vol. 35, no. 11, pp. 5179-5187, 2008.

[2] A. Aspradakis, J. Byrne, H. Palmans, J. Conway, K. Rosser, J. Warrington and S. Duane, "Small field MV photon dosimetry," IPEM Report No.103 (Institute of Physics and Engineering in Medicine), York, 2010.

[3] "Standards, Applications and Quality Assurance in medical radiation dosimetry (IDOS)," in *INTERNATIONAL SYMPOSIUM ON STANDARDS, APPLICATIONS AND QUALITY ASSURANCE IN MEDICAL RADIATION DOSIMETRY (IDOS)*, Vienna, Austria, 2010.

[4] T. Underwood, B. C. Rowland, R. Ferrand and L. Vieillevigne, "Application of the Exradin W1 scintillator to determine Ediode 60017 and microDiamond 60019 correction factors for relative dosimetry within small MV and FFF fields.," *Physics in Medicine and Biology,* vol. 60, no. 17, pp. 6669-6683, 2015.

[5] P. H. Charles, G. Cranmer-Sargison, D. I. Thwaites, S. B. Crowe, T. Kairn, R. T. Knight, J. Kenny, C. M. Langton and J. V. Trapp, "A practical and theoretical definition of very small field size for radiotherapy output factor measurements," *Medical Physics,* vol. 41, no. 4, pp. 041707-1-8, 2014.

[6] G. Cranmer-Sargison, P. H. Charles, J. V. Trapp and D. I. Thwaites, "A methodological approach to reporting corrected small field relative outputs," *Radiotherapy and Oncology,* vol. 109, pp. 350-355, 2013.

[7] S. Dieterich and G. W. Sherouse, "Experimental comparison of seven commercial dosimetry diodes for measurement of stereotactic radiosurgery cone factors," *Medical Physics,* vol. 38, no. 7, pp. 4166-4173, 2011.

[8] D. F. Lewis, "EBTXD_Specifications," Ashland Co..

[9] D. F. Lewis and M. F. Chan, "Technical Note: On GAFChromic EBT-XD film and the lateral response artifact," *Medcial Physics,* vol. 43, no. 2, pp. 643-649, 2016.

[10] S. Duane, "Dosimetry for Flattening Filter Free (FFF) linac beams and small fields (SF)," 2013.

[11] I. Čáp, "Small Field Dosimetry and FFF-Beam Technology," 2013.

[12] J. U. Wuerfel, "Dose Measurements in small fields," *Medical Physics International Journal,* vol. 1, no. 1, 2013.

[13] R. Alfonso, P. Andreo, R. Capote, M. S. Huq, W. Kilby, P. Kjall, T. R. Mackie, H. Palmans, J. Seuntjens, W. Ullrich and S. Vanitsky, "A new formalism for reference dosimetry of small and non standard fields," *Medical Physics,* vol. 39, p. 4009, 2008.

[14] H. Benmakhlouf, J. Sempau and P. Andreo, "Output correction factors for nine small field detectors in 6 MV radiation therapy photon beams: A Penelope Monte Carlo study," *Medical Physics,* vol. 41, no. 4, 2014.

[15] E. Chung, H. Bouchard and J. Seuntjens, "Investigation of three radiation detectors for accurate measurement of absorbed dose in nonstandard fields," *Medical Physics,* vol. 37, p. 2404, 2010.

[16] P. Carrasco and et al., "Characterization of the Exradin W1 scintillator for use in radiotherapy".

[17] D. S. Followill and et al, "The Radiological Physics Center's standard dataset for small field size output factors," *Journal of Applied Clinical Medical Physics,* vol. 13, no. 5, pp. 282-289, 2012.